Polar Biology
https://doi.org/10.1007/s00300-021-02940-2

ORIGINAL PAPER

Seasonal abundance, distribution, and growth of the early life stages of polar cod (*Boreogadus saida*) and saffron cod (*Eleginus gracilis*) in the US Arctic

A. L. Deary[1] · C. D. Vestfals[2] · F. J. Mueter[3] · E. A. Logerwell[1] · E. D. Goldstein[1] · P. J. Stabeno[4] · S. L. Danielson[5] · R. R. Hopcroft[5] · J. T. Duffy-Anderson[1]

Received: 26 August 2020 / Revised: 3 September 2021 / Accepted: 6 September 2021

Abstract

Polar cod and saffron cod are dominant components of the fish community in the Chukchi Sea and are ecologically important forage fishes linking plankton to upper-level consumers. In 2017, we conducted a study as part of the Arctic Integrated Ecosystem Research Program to characterize the distribution, abundance, and growth of polar cod and saffron cod early life history stages (ELHS) in late spring and late summer in the Chukchi Sea. Ship-based plankton tows showed that polar cod and saffron cod larvae were centered in Kotzebue Sound in the late spring. By late summer, polar cod juveniles were most abundant in the offshore areas of the northern Chukchi Sea, whereas saffron cod were distributed nearshore in the southern Chukchi Sea around Cape Lisburne. Empirical fish collections were paired with an individual-based biophysical transport model to examine connectivity and relate changes in seasonal distribution to potential environmental variables. Modeled drift trajectories and growth in spring for polar cod and saffron cod matched well with empirical observations, especially along the northern coastline of Kotzebue Sound, offshore of Point Hope/Cape Lisburne. Given the coherence between modeled and observed distributions, Kotzebue Sound is likely a source of gadid ELHS in the nearshore areas of the Chukchi Sea and offshore of Cape Lisburne/Point Hope, although it is not the likely source of polar cod over Hanna Shoal in the late summer. This is the first study to examine seasonal distribution, abundance, and growth of polar cod and saffron cod in the US Arctic and provides data necessary to evaluate the impacts of climate change on forage fishes in the Arctic.

Keywords Gadidae · Ichthyoplankton · Forage fishes · Chukchi Sea · Arctic cod

Introduction

The Arctic has experienced accelerated warming at twice the rate of the global average, making Arctic ecosystems particularly sensitive to climate change (Graham et al. 2017; Tokinaga et al. 2017; Overland et al. 2018). The accumulation of heat in the Arctic has increased significantly since the late 1990s, which correlates to a reduction in sea ice thickness (Maslowski 2014), a 60% loss of multiyear ice, a 75% reduction in sea ice volume (Overland et al. 2018), and lower winter ice extent maxima (Graham et al. 2017). Loss of sea ice is expected to influence Arctic ecosystem dynamics through bottom-up changes to lower trophic production (Kahru et al. 2011), community structure (Spear et al. 2019), trophic linkages (Hunt et al. 2013), shifts in benthic-pelagic coupling (Grebmeier et al. 2015 and citations therein), and food web interactions (Li et al. 2009). Ecosystem changes also have potential economic ramifications such as range

✉ A. L. Deary
alison.deary@noaa.gov

[1] Alaska Fisheries Science Center, NOAA, 7600 Sand Point Way NE, Seattle, WA 98115, USA

[2] Hatfield Marine Science Center, College of Fisheries and Ocean Sciences, University of Alaska Fairbanks, Newport, OR 97365-5229, USA

[3] College of Fisheries and Ocean Sciences, University of Alaska, 17103 Point Lena Loop Rd., Juneau, AK 99801-8344, USA

[4] Pacific Marine Environmental Laboratory, NOAA, 7600 Sand Point Way NE, Seattle, WA 98115, USA

[5] College of Fisheries and Ocean Sciences, University of Alaska Fairbanks, Fairbanks, AK 99775-7220, USA

Published online: 16 September 2021

extensions of commercially important subarctic gadid species, such as walleye pollock (*Gadus chalcogrammus*), Pacific cod (*Gadus macrocephalus*), and salmonid fishes, into regions north of the Bering Strait (Falardeau et al. 2017; Stevenson and Lauth 2019) in the Pacific Arctic.

Although not fished commercially in the US Arctic (NPFMC 2009), polar cod (*Boreogadus saida*), a circumpolar species, and saffron cod (*Eleginus gracilis*) are crucial forage fishes in Arctic marine ecosystems. Both species support bioenergetic pathways that transfer energy from planktonic food webs to upper-level consumers and apex predators (including humans) and are a dominant component of the fish community in the Chukchi Sea, although polar cod is more abundant than saffron cod (Whitehouse et al. 2014; Logerwell et al. 2015). It is estimated that seabirds and marine mammals consume approximately 75% of the polar cod production (Whitehouse et al. 2014). Changes to the Chukchi shelf ecosystem due to climatic warming, loss of sea ice, and perturbations to sea ice phenology (Graham et al. 2017; Overland et al. 2018) may have serious implications for these ecologically important species.

Despite their ecological importance and abundance in Arctic ecosystems, the life history of polar cod and saffron cod are still relatively unknown (Logerwell et al. 2015; Vestfals et al. 2019). Spawning locations of polar cod in the US Arctic are largely unknown, although it is hypothesized that polar cod spawn under sea ice (Rass 1968) and that peak hatching likely occurs in May and June as the ice edge recedes (Bouchard and Fortier 2008; Vestfals et al. 2019). In the Pacific Arctic, development of larvae and early juveniles occurs along the shelf (Logerwell et al. 2015; Vestfals et al. 2019). Saffron cod are near-shore, demersal, under-ice spawners that deposit demersal eggs in nearshore areas on sandy-pebbly substrates (Vestfals et al. 2019 and citations therein) but exact locations are unknown in the US Arctic. Peak hatching for saffron cod occurs in April and May, earlier than for polar cod, and offspring are often found concentrated closer to shore and at more southerly locations within the Chukchi Sea (Vestfals et al. 2019). The life histories of polar cod and saffron cod are similar in that both are planktonic in shelf waters after hatching through the first summer, after which polar cod move deeper in the water column while saffron cod become demersal as juveniles (Logerwell et al. 2015; Vestfals et al. 2019).

Growth of polar cod and saffron cod is mediated by temperature (Laurel et al. 2016) and an additional consequence of a warming Arctic is that large calanoid copepod species, an important prey resource for Arctic gadids, will be replaced by smaller, less lipid-rich copepods (Aarflot et al. 2018; Møller and Nielsen 2020; Bouchard and Fortier 2020). Larvae and juveniles will be disproportionally affected by these changes relative to adults due to their higher weight-specific growth rates, and polar cod may be more sensitive than saffron cod because they are a stenothermic species (Laurel et al. 2016). Polar cod are adapted to support high growth and lipid allocation at a narrow range of low temperatures (optimal growth rate at 5 °C), while saffron cod experience high growth and lipid allocation over a wider temperature range, particularly, at high temperatures (optimal growth rate > 16 °C) (Copeman et al. 2016; Laurel et al. 2016). As such, saffron cod may be better able to mitigate the effects of ocean warming in the Arctic than polar cod.

In 2017, the Arctic Integrated Ecosystem Research Program (Arctic IERP), funded by the North Pacific Research Board, conducted its first field season in the US Pacific Arctic. Concurrent with the Arctic IERP surveys, the Distributed Biological Observatory (DBO) project and the Arctic Marine Biodiversity Observation Network (AMBON) survey were also sampling the region, providing more coverage to this region that is often under-researched. In this inaugural year of sampling for the Arctic IERP, it was remarkable that the northern Bering Sea and Chukchi Sea were sampled for ichthyoplankton in both late spring and late summer, a first in the region. These sampling efforts provided an opportunity to assess the seasonal abundance, distribution, and growth of fishes during their early life history stages (ELHS). However, the summer of 2017 in the Chukchi Sea was also remarkable in environmental conditions, with an elevated sea surface temperature (+4 °C relative to the historic average) and the lowest recorded March sea ice minimum in the 39-year history of the time series (Perovich et al. 2017; Timmermans et al. 2017), providing us with baseline vital rate data for polar cod and saffron cod, albeit during a warm year. Such baseline data, when coupled with further monitoring and modeling, can be used to determine the impact of climate warming on these two ecologically important species. In addition to empirical sampling, we used an individual-based model (IBM) as a tool to simulate larval transport and examine potential linkages and connectivity in polar cod and saffron cod abundance and distribution between the late spring and late summer sampling events. Our goals for this study were to (1) examine spatial patterns of distribution and abundance of polar cod and saffron cod during their larval (June; late spring) and early juvenile (August–September; late summer) stages in 2017; (2) assess the change in mean length to approximate daily growth rates in the summer for polar cod and saffron cod; and (3) evaluate potential sources of larval polar cod and saffron cod using an IBM to compare observed distributions and sizes with model output. This study coupled empirical observations with IBM output to synthesize, for the first time, the seasonal distribution, abundance, and growth of two co-occurring Arctic forage fishes, providing a means to assess the biological impacts of warming on polar cod and saffron cod ELHS.

Methods

Specimen collection

Polar cod and saffron cod ELHS were collected in 2017, using three different sampling gears, as part of several cooperating research projects (Table 1): the Arctic Integrated Ecosystem Survey (AIES; part of Arctic IERP), AMBON survey, the Arctic Shelf Growth, Advection, Respiration, Deposition (ASGARD; part of Arctic IERP) project, and the DBO project. Larval and early juvenile Arctic gadids were targeted with a 60-cm bongo (bongo hereafter) equipped with a flow meter and a 505-µm mesh net fished obliquely from 10 m off the bottom or a maximum depth of 200 m to the surface in the late spring and late summer during the AIES and DBO surveys and to 5 m off the bottom or a maximum depth of 200 m for ASGARD. Demersal juvenile Arctic gadids (age-0, age-1 +) were targeted with a benthic-sampling 3-m plumb-staff beam trawl (Abookire and Rose 2005) equipped with 7-mm mesh and a 4-mm cod end liner during the late summer AMBON and AIES surveys (Table 1). The beam trawl was deployed from the stern of the vessel and towed at 1.5–2.0 knots for four minutes (Logerwell et al. 2015). Juvenile gadids (age-0, age-1 +) were also collected from the midwater during AMBON using a 1.5 m wide by 1.8 m high Isaacs-Kidd Midwater Trawl Net (IKMT) equipped with 3-mm mesh and a flowmeter (Table 1). The IKMT was towed double obliquely at 3.5–4.0 knots and these data were used to look at length and growth of Arctic gadids in August, prior to the late summer AIES surveys.

All bongo samples were fixed at sea in 5% formalin buffered with seawater and processed at the Plankton Sorting and Identification Center in Szczecin, Poland. ELHS of all fishes were identified to species, enumerated, and up to 50 specimens per taxon at each station were measured to the nearest 0.1 mm. Since specimens were measured after formalin fixation, we applied a + 1.9% correction factor to the measured lengths to account for shrinkage (D. Blood, B. Laurel, NOAA, unpublished data; Vestfals et al. 2019). The identifications of ELHS gadids were verified by scientists at the National Oceanic and Atmospheric Administration's Alaska Fisheries Science Center using Matarese et al. (1989), Dunn and Vinter (1984), and Ichthyoplankton Information System IIS (2019). Due to concerns of Walleye Pollock (*Gadus chalcogrammus*) being misidentified as Polar Cod, the Arctic gadids captured during AIES using the beam trawl were verified using genetic methods following Wildes et al. (2016). No specimens of juvenile Arctic cod (*Arctogadus glacialis*) were detected (S. Wildes, Alaska Fisheries Science Center (AFSC), personal communication), suggesting that *A. glacialis* was not present in our study region since the abundance of later stages is reflective of the abundance of the earlier stages (Bouchard et al. 2016).

Catch per unit effort of polar cod and saffron cod was reported as the number of individuals caught under a sea surface area of 10 m^2 (count per 10 m^2). Trawl samples (IKMT and beam trawl) were processed at sea with all individual fishes being identified, enumerated, and measured to the nearest length in millimeters. Standard length (SL) was measured for individuals at flexion size or larger and notochord length (NL) for individuals smaller than flexion. The reported size of flexion is 11.0 mm for polar cod and saffron cod (IIS 2019). Catch for the AIES and AMBON beam trawl was expressed as number of individuals caught per unit area swept (count per 1000 m^2).

Data analysis

All catch and length data were analyzed using R (ver. 3.5.2; R Core Team 2019). For the length data, to account for only a subset of larvae being measured ($n = 50$ maximum), the estimated proportion of individuals at each length was multiplied by the standardized catch at that station (catch-weighted length). Individuals of polar cod and saffron cod larger than 70 mm SL were presumed to be one year or older based on a cutoff identified in the length–frequency distribution and were excluded from the subsequent length analyses.

Table 1 Arctic Integrated Ecosystem Research Program 2017 sampling events in the northern Bering and Chukchi Seas

Survey identifier	Sampling program	Dates	Season	# of samples	Gear used
SQ17-01	ASGARD*	10–29 June	Late spring	61	60BON
NM17-01	AMBON	4–23 August	Late summer	75	PSBT
				13	IKMT
OS17-01	AIES*	8 August–25 September	Late summer	72	60BON
				62	PSBT
HE17-02	DBO*	29 August–10 September	Late summer	64	60BON

AIES Arctic Integrated Ecosystem Survey, *AMBON* Arctic Marine Biodiversity Observation Network, *ASGARD* Arctic Shelf Growth, Advection, Respiration, Deposition, *DBO* Distributed Biological Observatory, *60BON* 60-cm bongo, *IKMT* Isaacs-Kidd Midwater Trawl, *PSBT* 3-m plumb-staff beam trawl

Asterisks (*) denotes programs affiliated with Arctic Integrated Ecosystem Research Program

Our use of 70 mm SL to delineate between age-0 and age-1 polar cod is smaller than the size of this transition identified in prior work determining length at age using otoliths [84.0 mm fork length (FL) and 81.6 mm total length (TL), respectively] (Craig et al. 1982; Lønne and Gulliksen 1989) because standard length excludes measuring the caudal fin rays that are often damaged during collection. The transition of saffron cod from age-0 to age-1 is not as definitive as that for polar cod due to an overlap in size at these ages occurring between 55 and 110 mm FL in the Chukchi Sea (Wolotira 1985; Copeman et al. 2016; Helser et al. 2017). However, in Arctic samples collected in 2012 all individuals greater than 75 mm FL were age-1 based on otolith analyses, suggesting our size cutoff is reasonable for the region sampled (Copeman et al. 2016). Specimens were then aggregated into 2-mm length bins. For the AMBON samples collected with the IKMT and the beam trawl, subsamples of fish were measured to the nearest millimeter. Many of the smallest individuals (less than 50 mm) were not measured and were instead sorted into approximate 10-mm size bins, enumerated in the field, and then discarded. The binned individuals were combined with the measured individuals by simulating individual lengths of the binned individuals from a uniform random distribution within their assigned size bin. Other distributions (normal, beta) were considered for simulating lengths of the binned individuals but had minimal impact on the resulting length-frequencies.

Daily growth rates were estimated for each species as the change in mean length from June 19th, 2017, the median date of the late spring (June) ASGARD survey, and each late summer survey (AMBON and AIES) under the assumption that these individuals were from the same cohort. The median date of the AMBON survey was August 13th, 2017 and the median date of the AIES survey was September 1st, 2017. Mean length for late spring was based on all individuals collected during the survey using the bongo. Mean length for the late summer individuals was gear-specific and calculated based on all putative age-0 specimens collected during: (1) AMBON survey using a beam trawl, (2) AMBON survey using an IKMT, (3) AIES and DBO surveys using a bongo, and (4) AIES survey using a beam trawl. Data for these growth analyses did not include estimates from midwater-collected gadids sampled during the late summer AIES and DBO surveys, but they were available from the IKMT fished during the 2017 late summer AMBON survey, providing some estimates of growth of midwater-associated fishes. Daily growth rates are presented as a range; the estimate provided from the late summer bongo collections represents a low estimate as larger gadids tend to escape from the bongo net (Shima and Bailey 1994) and likely represents individuals that are smaller-than-average. Late summer beam trawl collections (AIES) represent a high growth estimate as the coarser mesh size of the trawl may select for larger individuals that are larger-than-average and generally resulted in the greatest mean size. For polar cod, length-dependent mortality results in slightly greater length at age estimates (Thanassekos et al. 2012), suggesting our study will be overestimating growth since we are relying on changes in length of survivors (those individuals captured and measured by the various gear types) to estimate growth. A daily growth rate was also calculated using the IKMT data to explore differences in the apparent growth rates between age-0 fishes that are still pelagic and those that have become demersal by the time of sampling. We expected the apparent growth rate to increase as individuals become more demersal. Size distribution from the IKMT and beam trawl are likely to be directly comparable as the IKMT mesh size (4 mm) was identical to that of the beam trawl liner.

Densities (catch per unit area) of polar cod and saffron cod were mapped to explore the seasonal distribution of ELHS of Arctic gadids in the northern Bering and Chukchi seas relative to sea ice concentration on June 19th and September 1st, 2017. Sea ice concentrations were obtained from the National Snow and Ice Data Center at 25 km by 25 km spatial resolution (Cavalieri et al. 1996; NSIDC 2019).

Individual-based biophysical model for polar cod and saffron cod

Late spring and late summer distributions were compared to simulated distributions from biophysical transport models parameterized for polar cod and saffron cod larval and early juvenile stages (Vestfals et al. 2021). Details on the model parameterization and the results of validation testing are described in Vestfals et al. (2021). These models were developed to simulate the growth and dispersal of early life stages in the northern Bering, Chukchi, and Beaufort seas to identify possible spawning locations, which are largely unknown, as well as to examine gadid connectivity between these seas. An implementation of the Regional Ocean Modeling System (ROMS) (Shchepetkin and McWilliams 2005) set up in a Pan-Arctic (PAROMS) configuration (Danielson et al. 2016) was used to realistically simulate the three-dimensional (3-D) circulation field. PAROMS has a horizontal resolution of ~ 5 km south of the Aleutian Islands to 9 km in the North Atlantic and is approximately 5.5–6.0 km in the Chukchi Sea, and is forced by the Japanese 55-year atmospheric reanalysis JRA55-do (version 1.4) (Tsujino et al. 2018), which also provides estimates of freshwater runoff. Boundary conditions come from the Simple Ocean Data Assimilation (SODA) reanalysis (version 3.3.1) (Carton et al. 2018) prior to 2015 and the Hybrid Coordinate Ocean Model (HYCOM) (Chassignet et al. 2009) for more recent years. The Oregon State TOPEX/Poseidon Global Inverse Solution (Egbert and Erofeeva 2002) provides tidal forcing and the sea ice field is based on the single-category

Budgell ice model (Budgell 2005). To simulate advection and growth of larvae, IBMs for polar cod and saffron cod were developed using the particle tracking tool TRACMASS that calculates Lagrangian trajectories from Eulerian velocity fields (Döös 1995).

Stage-specific and size-specific temperature-dependent growth rates were used to model the growth of polar cod and saffron cod (Porter and Bailey 2007; Laurel et al. 2016; Koenker et al. 2018) to 45 mm in length, the size at which these species are thought to transition from pelagic juveniles to more demersal juveniles, with enhanced swimming abilities. In addition, these stages correspond most closely to the stages captured by the water column sampling gear (bongo and IKMT) during the field campaign allowing for comparison between simulated and observed distributions of the two species. Similar to the growth rates calculated for the 2017 empirical data, mean daily growth rates were estimated for the simulated larvae for each species as the change in mean length from late spring (June 19th) to late summer (September 1st) divided by the number of days elapsed.

Hatching locations were identified through a thorough literature review, anecdotal evidence, and known areas of retention in the Pacific Arctic (Vestfals et al 2021 and references therein). However, due to the preponderance of early-stage individuals encountered in the Kotzebue Sound region during spring 2017, we focused this study on this region as a potential source of polar cod and saffron cod in the US Chukchi Sea. For our study, Kotzebue Sound will include the area that extends from the northwestern tip of Seward Peninsula to Point Hope. Simulations were initialized from all PAROMS grid points falling within the eastern-most part of Kotzebue Sound as hatching location (Fig. 1), with 10 particles released per 5 m depth increment to the bottom at each PAROMS grid point. The Chukchi Sea is often shallower than 40 m, which represents the maximum release depth of particles in the model (Vestfals et al. 2021). Based on results from initial particle simulations, dispersal simulations were conducted with larvae hatching on the 1st and 15th day of each month from March 1st to May 15th, for a total of six hatching events. Temperature-mediated growth and dispersal of larvae were simulated until September 1st, the midpoint of the late summer Arctic field surveys in 2017, so that the simulated distribution and size composition during summer could be compared to the observed distributions and size compositions of individuals captured during the surveys.

IBM parameterization-polar cod

Several vertical behaviors were developed for polar cod based on available literature (Borkin et al. 1986; Bouchard et al. 2016) and from laboratory observations (B. Laurel, AFSC, *unpublished data*). Of the five different vertical behavior routines tested, simulations with surface-oriented individuals, where all stages were found at 5 m matched best with prior field observations from acoustic-trawl surveys conducted in 2012 and 2013 (DeRobertis et al. 2017; Vestfals et al. 2021). Polar cod growth was based on growth equations described in Koenker et al. (2018) and Laurel et al. (2016). Simulated larval sizes and distributions on June 19th (midpoint of the ASGARD survey) and September 1st (midpoint of AIES) from simulations originating in Kotzebue Sound were compared to field observations.

IBM parameterization-saffron cod

Similar vertical behaviors were used for the saffron cod simulations as for polar cod since no information on the vertical distribution of saffron cod larvae is available at present. Preflexion larval growth from hatch to 10 mm in length was based on temperature-dependent growth experiments (B. Laurel, unpublished data; Vestfals et al. 2021). At present, temperature-dependent growth models for saffron cod ELHS > 10 mm in length are not available. As growth of saffron cod at these small sizes is linear and resembles that of walleye pollock (B. Laurel, AFSC, unpublished data), the growth model described in Porter and Bailey (2007) was used to model saffron cod growth from 10 to 45 mm.

Results

Field data

Sea ice

As of June 1st, just prior to the survey, sea ice was present in the Kotzebue Sound region (S. Danielson, University of Alaska Fairbanks (UAF), unpublished data). By June 19th, the mid-point of the late spring survey, sea ice was receding and the entire survey area was ice-free.

Abundance, distribution, and size of polar cod

In June, the highest densities of polar cod (> 640 individuals per 10 m^2) were found at nearshore stations of Kotzebue Sound and Point Hope transects and along the entire Cape Lisburne transect (Fig. 2a). Polar cod density was lower south of the Bering Strait with most individuals being encountered along the northernmost transects sampled in the Chukchi Sea. By late summer (August and September), sea ice remained absent in the survey region south of 75°N, except in the nearshore area of Kotzebue Sound. The overall density of polar cod decreased from an average catch of 1183 individuals per 10 m^2 in the late spring to 7 individuals per 10 m^2 in the late summer in the

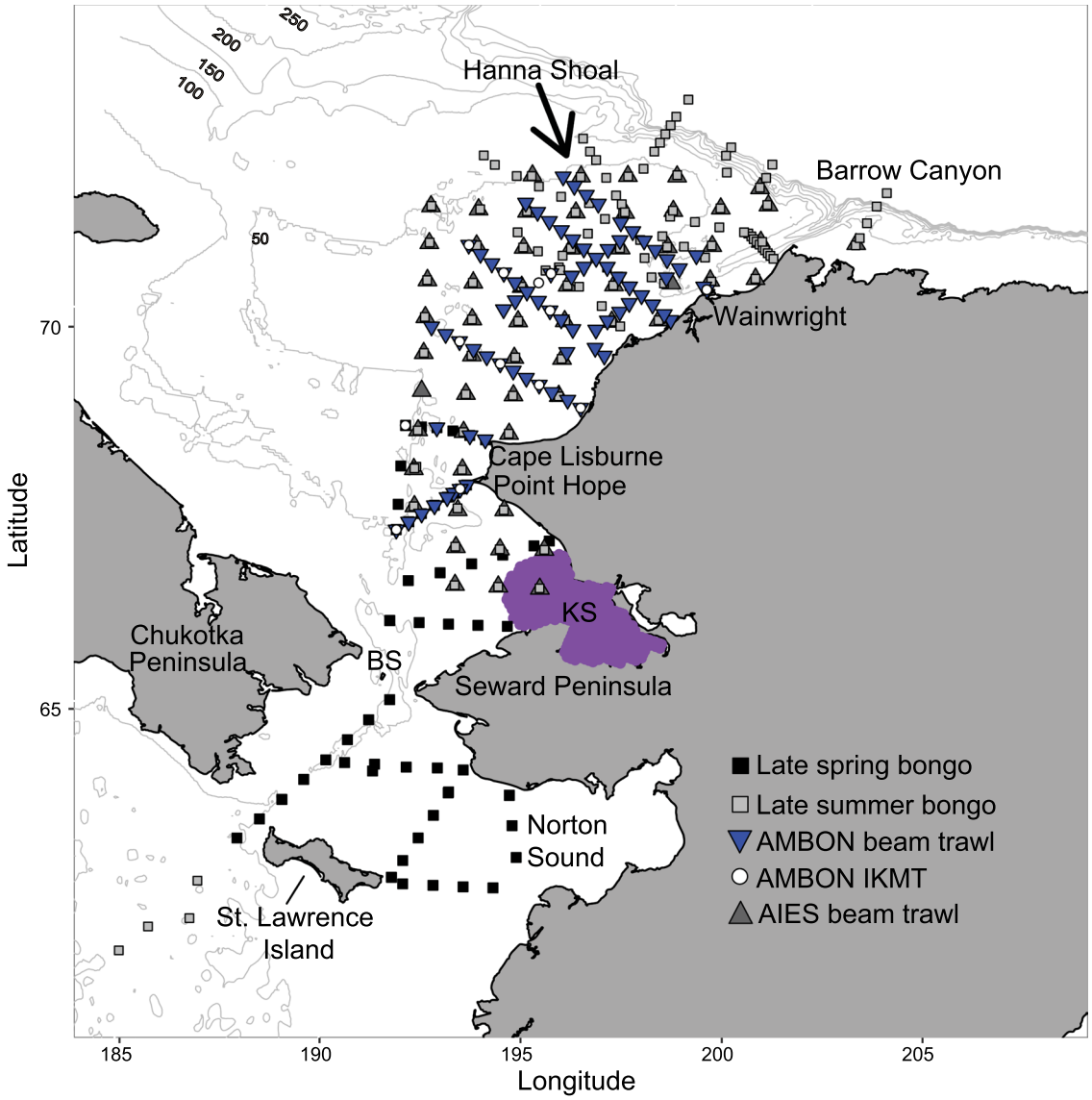

Fig. 1 Survey stations sampled in 2017 in the Chukchi Sea, Bering Strait (BS), and northern Bering Sea. Bongo –Late spring black squares and late summer (August/September) gray squares; beam trawl–AMBON survey (August) blue inverted triangles and AIES (August/September) dark gray triangle; and Isaacs-Kidd Midwater Trawl (IKMT) –AMBON survey (August) white circles. Simulated release locations from the individual-based model in the eastern-most area of Kotzebue Sound (KS), which is shaded in purple. Kotzebue Sound also refers to the broader region from the northwestern tip of Seward Peninsula and Point Hope to the north. Depth contours extend from 50 to 250 m in 50 m increments

water column. The highest densities of polar cod in the water column (> 10 individuals per 10 m^2) were observed in the northern portion of the survey area in the late summer, particularly around Barrow Canyon and Hanna Shoal (Fig. 2b). The distribution of polar cod in the water column was similar to the distribution of demersal individuals. Demersal catches of juvenile polar cod (< 70 mm SL) were highest offshore in the northern Chukchi Sea in the late summer in areas where bottom water temperatures were below approximately 5 °C (Fig. 3a and b).

In June, the mean length of polar cod larvae in the water column was 9.8 mm NL ($n = 850$), with most larvae being less than 12.0 mm in length (Fig. 4a; Table 2). By the end of the summer, the length distribution of polar cod had expanded and the mean length increased to 30.1 mm SL ± 0.9 ($n = 140$) and 30.7 mm SL ± 0.4 ($n = 433$) for specimens collected in the water column with the bongo and IKMT gears, respectively (Fig. 4c, e; Table 2). In late summer (August–September) the mean length of demersal polar cod was 39.7 mm SL ± 0.4 ($n = 718$) in the AMBON

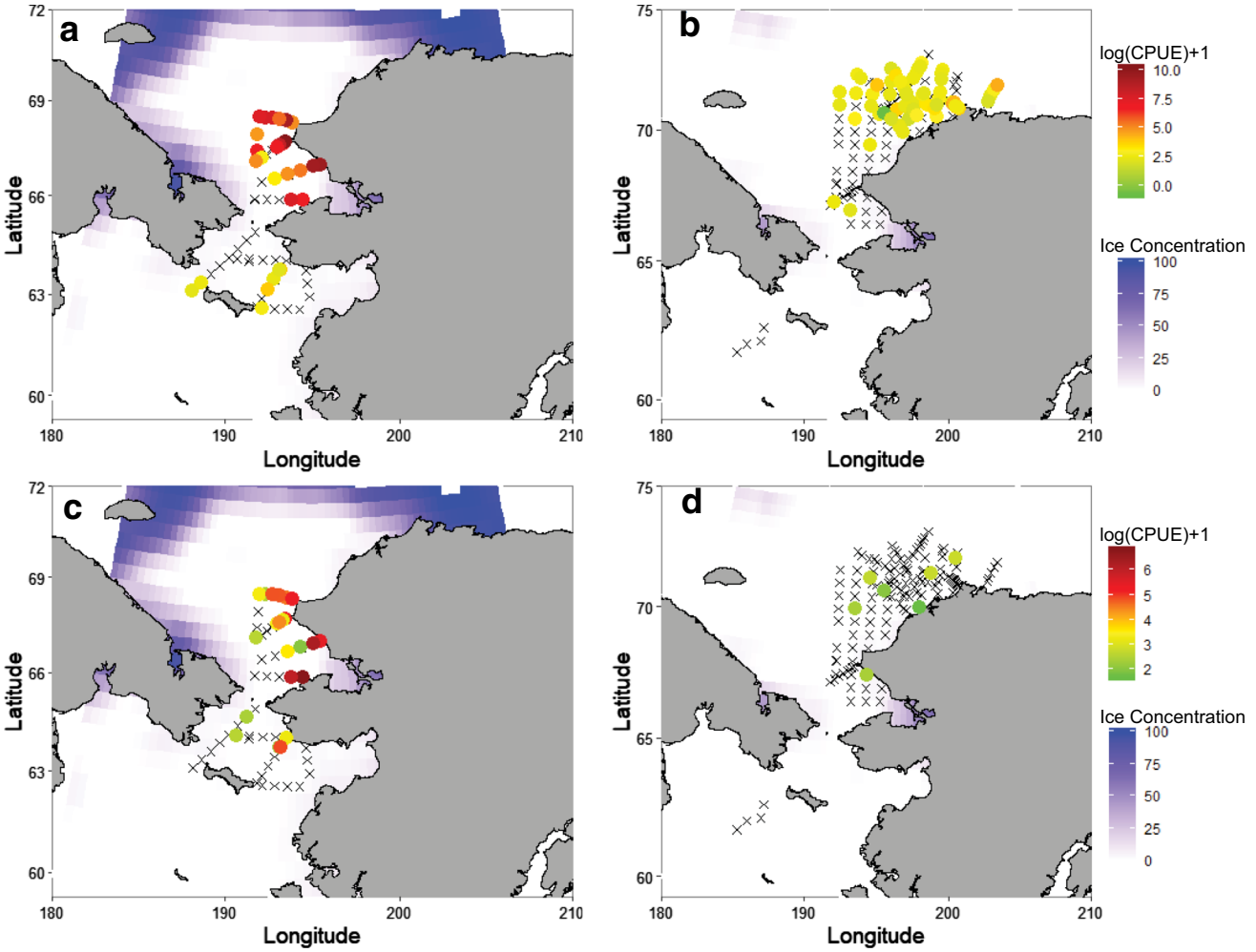

Fig. 2 Distribution of polar cod (*Boreogadus saida*) (**a**, **b**) and saffron cod (*Eleginus gracilis*) (**c**, **d**) in late spring (left column) and late summer (right column) 2017 collected in the water column with the 60-cm bongo net. Catch data are reported as catch-per-unit-effort (CPUE) and log(CPUE) + 1 to highlight variability at lower abundances. Ice concentration (% cover) is plotted in the background. Black X's denote sampled stations where polar cod and saffron cod were not caught. Note the different scales for CPUE between the species

beam trawl samples and 47.8 mm SL ± 1.6 ($n = 690$) in the AIES beam trawl samples (Fig. 4g, i; Table 2). Based on changes in length and an assumption that larvae collected in the late summer surveys were from the same cohort as fish collected in the late spring, the estimated daily growth rate for polar cod during 2017 ranged from 0.27 mm day^{-1} based on individuals in the water column to 0.53 mm day^{-1} based on individuals that had become demersal (Table 3), with an overall mean of 0.39 ± 0.06 mm day^{-1} ($n = 4$) based on all measured individuals.

Abundance, distribution, and size of saffron cod

The density of pelagic larval saffron cod in June was highest at the nearshore stations in Kotzebue Sound and Cape Lisburne, which were both ice covered on June 1st, prior to the mid-point of the survey, with densities ranging from 68 to 444 individuals per 10 m^2. The highest observed density of saffron cod was at the innermost station along the southern margin of Kotzebue Sound (Fig. 2c). Catches south of Kotzebue Sound were low (less than 30 individuals per 10 m^2). Densities of saffron cod were much lower later in the summer (August and September), with most of the stations yielding no saffron cod (Fig. 2d). Unlike saffron cod in the water column, demersal larval and early juvenile saffron cod in later summer were rarely encountered offshore, with most individuals concentrated near Cape Lisburne (Fig. 3c and d). Demersal saffron cod were observed in areas with higher bottom temperatures than demersal polar cod. In early August, saffron cod were concentrated in areas with bottom water temperatures greater

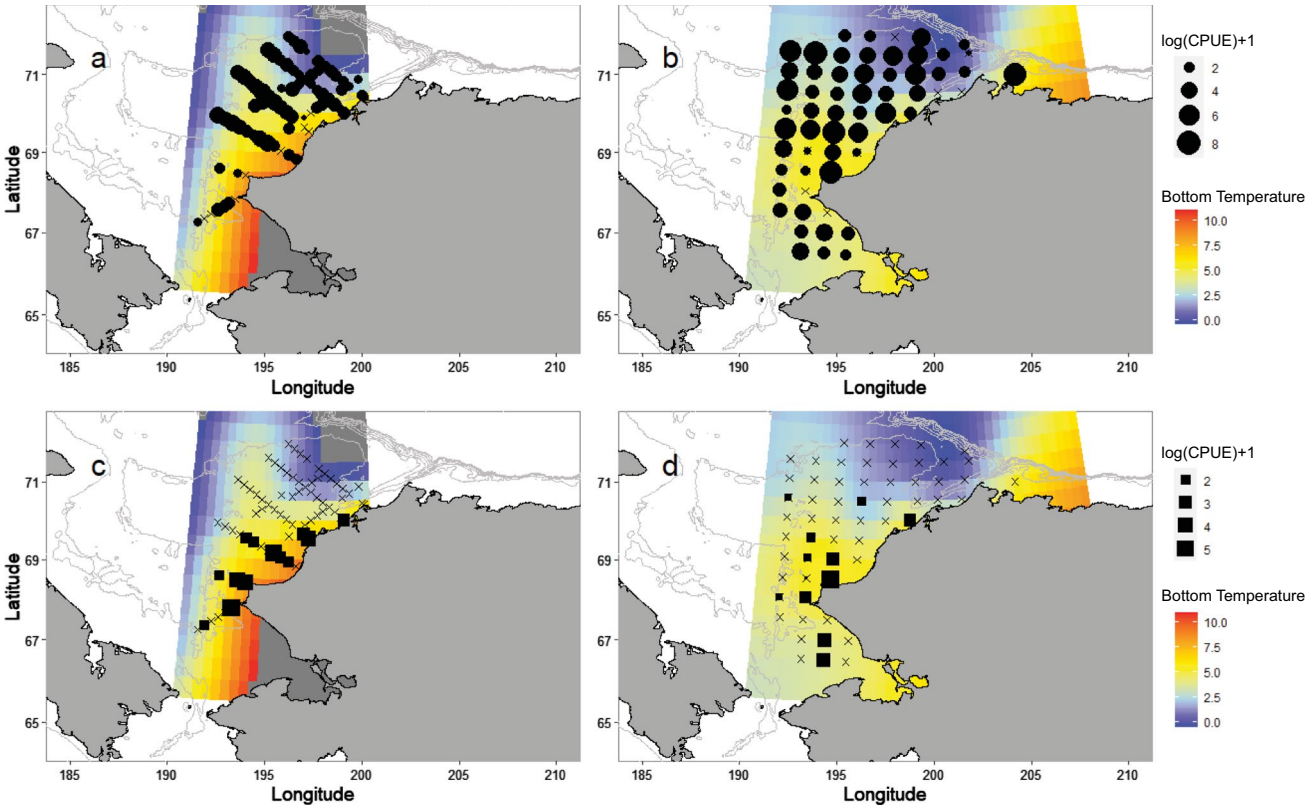

Fig. 3 Late summer distributions of demersal juvenile polar cod (*Boreogadus saida*) from AMBON (**a**) and AIES (**b**) beam trawl collections and of demersal juvenile saffron cod (*Eleginus gracilis*) from the AMBON (**c**) and AIES (**d**) beam trawl collections. The background color denotes bottom temperature in °C. Catch data are reported as catch-per-unit-effort (CPUE) and log(CPUE) + 1 to highlight variability at lower abundances. Note the different scales for CPUE between the species

than 7.5 °C and by September occupied areas with bottom water temperatures greater than 5.4 °C.

Saffron cod had a mean length of 9.3 mm NL ± 0.4 ($n = 299$) in June, with most individuals measuring less than 14.0 mm in length (Fig. 4b; Table 2). By late summer, the mean length of saffron cod ranged from 18.5 mm SL ± 1.4 ($n = 7$) in the bongo to 40.3 mm SL ± 1.7 ($n = 41$) in the IKMT (Fig. 4d, f). The mean length of demersal saffron cod was 51.6 mm SL ± 0.4 ($n = 318$) in the AMBON beam trawl and 55.1 mm SL ± 1.7 ($n = 54$) in the AIES beam trawl by late summer (Fig. 4h, j; Table 2). The daily growth rate for saffron cod was estimated as 0.12 mm day^{-1} to 0.76 mm day^{-1} (Table 3), with a mean of 0.37 ± 0.16 mm day^{-1} ($n = 4$).

Comparison of distribution and size of polar cod and saffron cod

Catches of saffron cod were lower relative to polar cod regardless of season. In June, the core distribution of saffron and polar cod overlapped in Kotzebue Sound, with polar cod found farther offshore than saffron cod (Fig. 2). Later in the summer, saffron cod were encountered in bongo samples of the water column at only 7 of the 136 stations sampled. Demersal juveniles of polar cod were observed farther offshore and to the north relative to saffron cod in the late summer. They were also most abundant offshore of the region between Cape Lisburne and Wainwright at stations with bottom water temperatures cooler than 5.0 °C. In contrast, demersal juveniles of saffron cod were most abundant nearshore off Cape Lisburne and in northern Kotzebue Sound where bottom water temperatures were warmer than 7.5 °C (Fig. 3b, d).

Polar cod and saffron cod were similar in mean size in June when their distributions also overlapped. Later in the season, far fewer saffron cod ($n = 420$) were captured and measured compared to polar cod ($n = 1981$). Demersal saffron cod were larger than those found in the water column in the late summer. The range of daily growth rates was wider for saffron cod than polar cod, but the mean daily growth rate was similar between saffron cod and polar cod at 0.37 ± 0.16 and 0.39 ± 0.06 mm day^{-1}, respectively ($n = 4$).

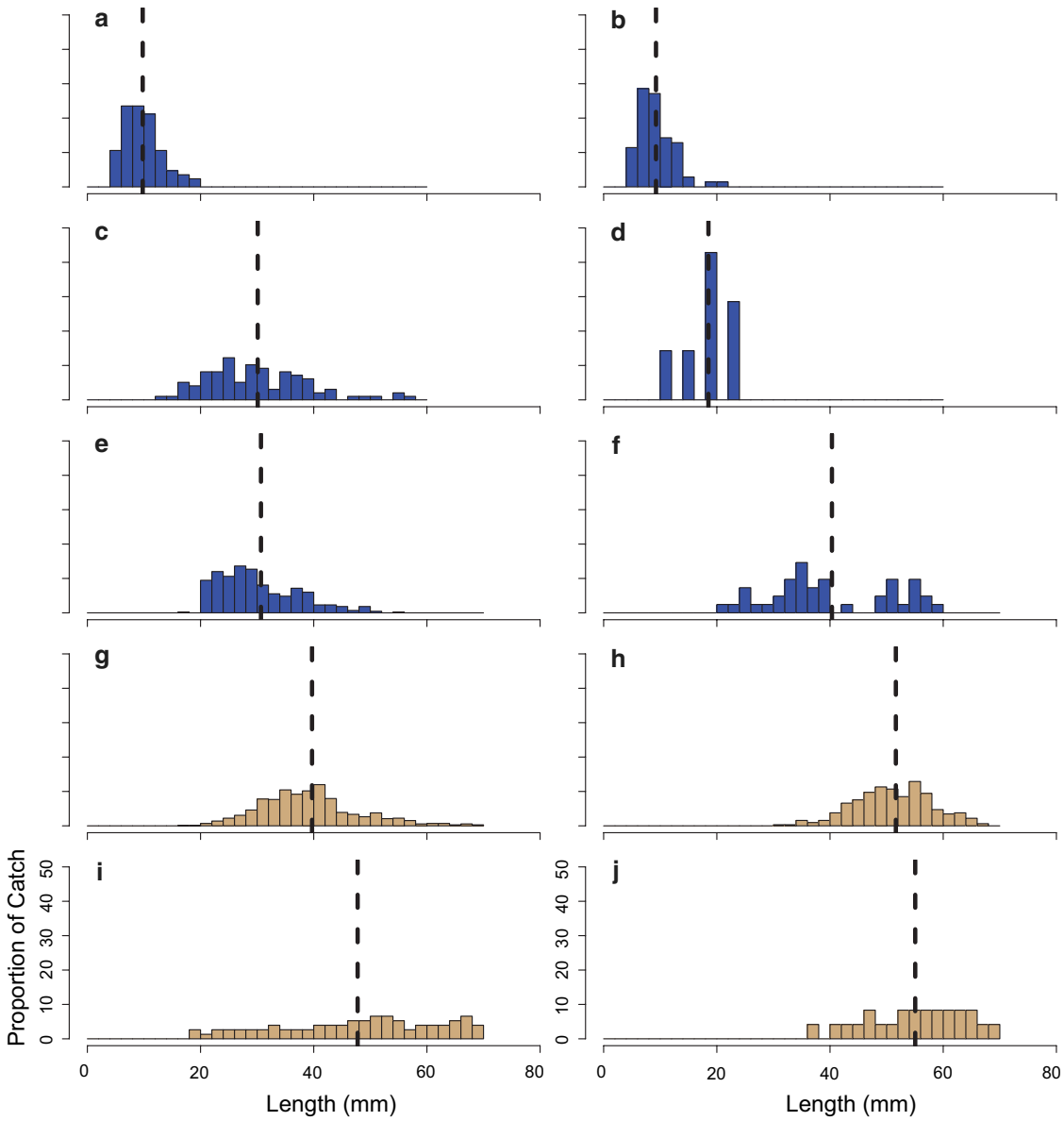

Fig. 4 Length distributions of polar cod (*Boreogadus saida*) (left) and saffron cod (*Eleginus gracilis*) (right) during the late spring (**a**, **b**) and late summer collections with 60-cm bongo (**c**, **d**), Isaacs-Kidd Midwater Trawl (IKMT) (**e**, **f**), AMBON beam trawl (**g**, **h**), and AIES beam trawl (**i**, **j**). Dotted black lines denote the mean length for each histogram. Blue bars represent individuals collected from the water column and brown bars represent those collected along the seafloor. Specimens are binned into 2-mm length intervals and standardized by CPUE when all captured individuals were not measured (i.e., bongo)

IBM simulated data

Simulated distribution and size of polar cod

On June 19th, simulated polar cod hatching in Kotzebue Sound between March 15th and May 15th had similar dispersal trajectories and were mostly found to be retained in and around Kotzebue Sound and in the nearshore region northward to Cape Lisburne (Fig. 5). At Cape Lisburne, some larvae were transported offshore to the north and to the west, and were concentrated in two different trajectories, except for simulated individuals hatched on May 15th. Other individuals were transported northward along the coastline. Based on the 2017 simulations, no individuals were transported to the south in the late spring, though polar cod were observed in the late spring survey around St. Lawrence Island (Fig. 2a; Fig. 5). By September 1st, simulated polar cod were found in the nearshore region from Kotzebue Sound north to Wainwright (Fig. 6). Simulated polar cod were advected offshore, almost due west, at Cape Lisburne/

Table 2 Late spring and late summer 2017 observed length data for polar cod (*Boreogadus saida*) and saffron cod (*Eleginus gracilis*)

Species	Late Spring	Late Summer			
	60BON	60BON	IKMT	AMBON Trawl	AIES Trawl
Polar cod	5.1 NL–19.7 (9.8 ± 0.4 NL, *n* = 850)	13.2–56.1 (30.1 ± 0.9, *n* = 140)	18.0–56.0 (30.7 ± 0.4, *n* = 433)	*18.0–69.0 (39.7 ± 0.4, n = 718)*	*18.5–69.8 (47.8 ± 1.6, n = 690)*
Saffron cod	4.7 NL–21.2 (9.3 ± 0.4 NL, *n* = 299)	11.4–22.4 (18.5 ± 1.4, *n* = 7)	22.0–59.0 (40.3 ± 1.7, *n* = 41)	*31.0–68.0 (51.6 ± 0.4, n = 318)*	*37.9–69.0 (55.1 ± 1.7, n = 54)*

Mean size, standard error, and sample size (*n*) are displayed within the parentheses. Demersal gears are emphasized in italics and all lengths are reported in mm and in standard length, unless noted otherwise

AIES Arctic Integrated Ecosystem Survey, *AMBON* Arctic Marine Biodiversity Observation Network, *60BON* 60-cm bongo, *IKMT* Isaacs-Kidd Midwater Trawl, *NL* notochord length

Table 3 Daily growth rate estimates (mm day^{-1}) for polar cod (*Boreogadus saida*) and saffron cod (*Eleginus gracilis*) in the Chukchi Sea between late spring and late summer

Species	60BON	IKMT	*AMBON Trawl*	*AIES Trawl*	Mean daily
Polar cod	0.27	0.37	*0.53*	*0.51*	0.39 ± 0.06 (*n* = 4)
Saffron cod	0.12	0.56	*0.76*	*0.61*	0.37 ± 0.16 (*n* = 4)

Demersal sampling gears are emphasized in italics

AIES Arctic Integrated Ecosystem Survey, *AMBON* Arctic Marine Biodiversity Observation Network, *60BON* 60-cm bongo, *IKMT* Isaacs-Kidd Midwater Trawl, *n* sample size

Point Hope. Hatch date did not greatly impact the end points of the simulated polar cod on September 1st (Fig. 6). In the late summer, simulated polar cod were abundant offshore of Cape Lisburne/Point Lay and Wainwright but uncommon nearshore along the coastline from Kotzebue Sound to Wainwright (Fig. 6), which was consistent with the empirical data (Fig. 2b; Fig. 3).

The mean size of simulated polar cod individuals hatched between March 1st and April 1st was larger than individuals captured in the field (Fig. 4, Fig. 7). Simulated individuals hatched on May 1st and May 15th were on average smaller than the field samples. For larvae that hatched on April 15th, the average size of simulated polar cod matched the average size of the captured individuals, although the range was broader for the individuals caught in the field compared to the simulated individuals (Table 2, Table 4). In the late summer, the average size of the simulated polar cod was smaller than the wild-caught specimens regardless of hatch date (Fig. 7). The simulated sizes were most similar to polar cod captured using the bongo in the late summer (Table 2, Table 4).

Simulated distribution and size of saffron cod

The simulated distribution of saffron cod in the late spring and late summer was similar to that of polar cod (Fig. 8). Similar to polar cod in the late spring, no simulated saffron cod larvae were found along the southern coastline of Kotzebue Sound, whereas saffron cod larvae were captured along the southern coastline of Kotzebue Sound and northern coastline of Norton Sound (Figs. 2–3). In the late summer, simulated saffron cod were densely concentrated along the coastline extending from Kotzebue Sound to just north of Wainwright with two offshore advection areas at Point Lay/Cape Lisburne and south of Wainwright (Fig. 9). Catches of saffron cod were low in the late summer but the areas with the highest catches corresponded to high density areas identified by the model, particularly offshore of Wainwright and Point Lay/Cape Lisburne (Figs. 2–3; 9).

Regardless of season or hatch date, simulated saffron cod were smaller on average than field captured individuals (Table 2, Table 4). In addition, the length range of simulated individuals was narrower than the captured individuals in the late spring and late summer (Fig. 10). Unlike simulated polar cod, there was little overlap in the late spring and late summer sizes of simulated saffron cod (Fig. 10). In the late spring, simulated saffron cod did not grow larger than 8.5 mm NL and had a mean size of 5.7 mm NL ± 0.0025–0.0037 for all simulated hatch dates (Fig. 10, Table 4). In the late summer, the average size of simulated saffron cod ranged from 14.6 mm SL ± 0.024 to 14.9 mm SL ± 0.023 (Fig. 10, Table 4).

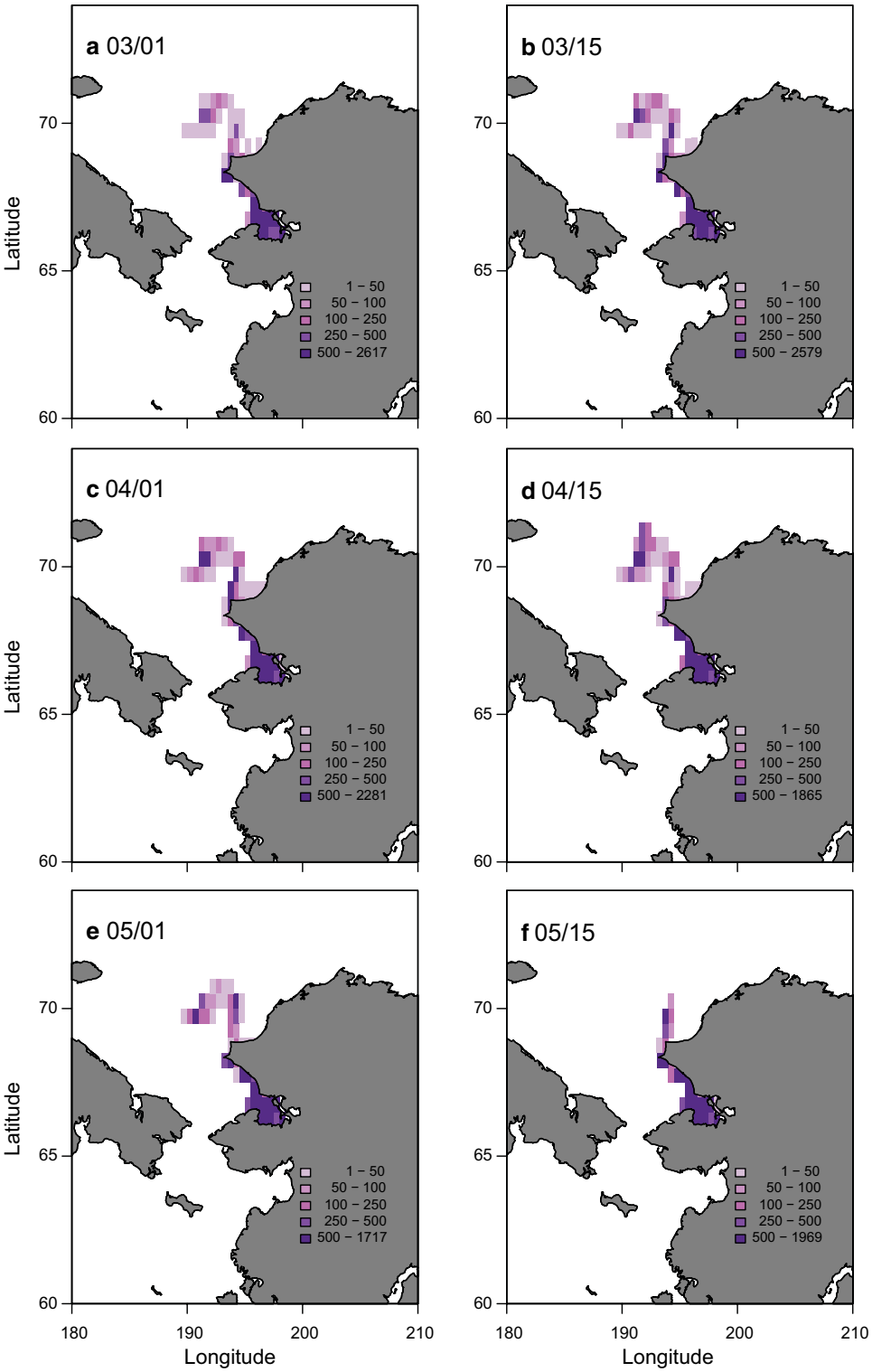

Fig. 5 Density of simulated endpoints from individual-based models in the late spring (June 19th, 2017) for polar cod (*Boreogadus saida*) larvae hatching in Kotzebue Sound. Hatch dates are: **a** March 1st, **b** March 15th, **c** April 1st, **d** April 15th, **e** May 1st, and **f** May 15th. Density is calculated in a 0.5 × 0.5 degree grid

Discussion

Spawning areas and drift

Sea ice was present in Kotzebue Sound at the approximate time of hatch for both polar cod and saffron cod until early June (S. Danielson, UAF, unpublished data; Cavalieri et al. 1996), suggesting that sea ice may be important for the newly hatched larvae of both species. Kotzebue Sound may indeed be a hatching area for polar cod and a source of juveniles to the north later in the summer. One of the main northward currents in the eastern Chukchi Sea is the Alaska

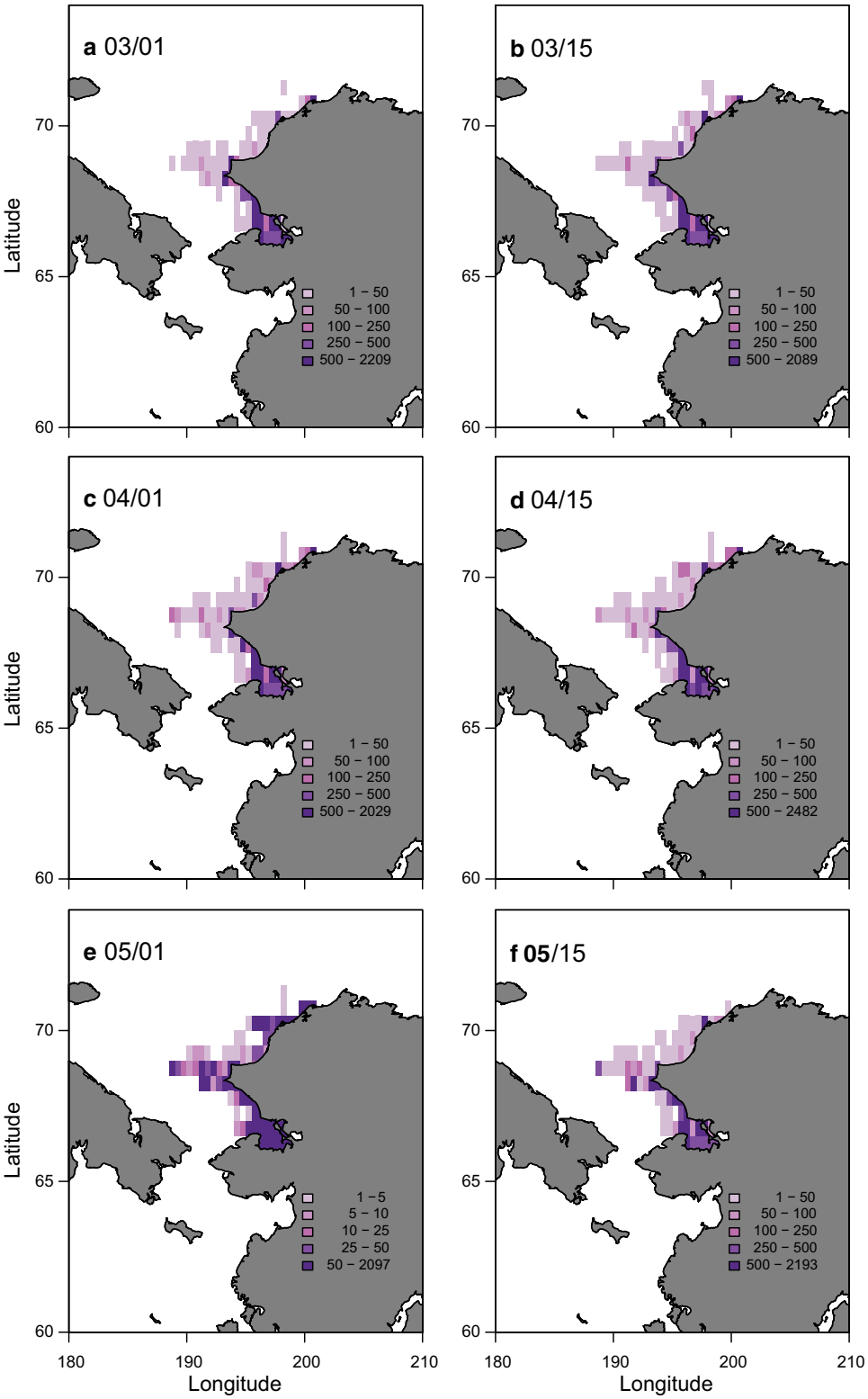

Fig. 6 Density of simulated endpoints from individual-based models in the late summer (September 1st, 2017) for polar cod (*Boreogadus saida*) hatching in Kotzebue Sound. Hatch dates are: **a** March 1st, **b** March 15th, **c** April 1st, **d** April 15th, **e** May 1st, and **f** May 15th. Density is calculated in a 0.5 × 0.5 degree grid

Coastal Current (ACC), which flows through Bering Strait and past the mouth of Kotzebue Sound and it is likely to entrain larvae originating in the Sound. Transport through Bering Strait has been increasing in recent years, which, in turn, has increased heat transport into the Chukchi Sea and the rate of sea ice retreat in the spring (Woodgate et al. 2012; Woodgate 2018), as well as current velocity that may increase the dispersal potential for ELHS entrained in the

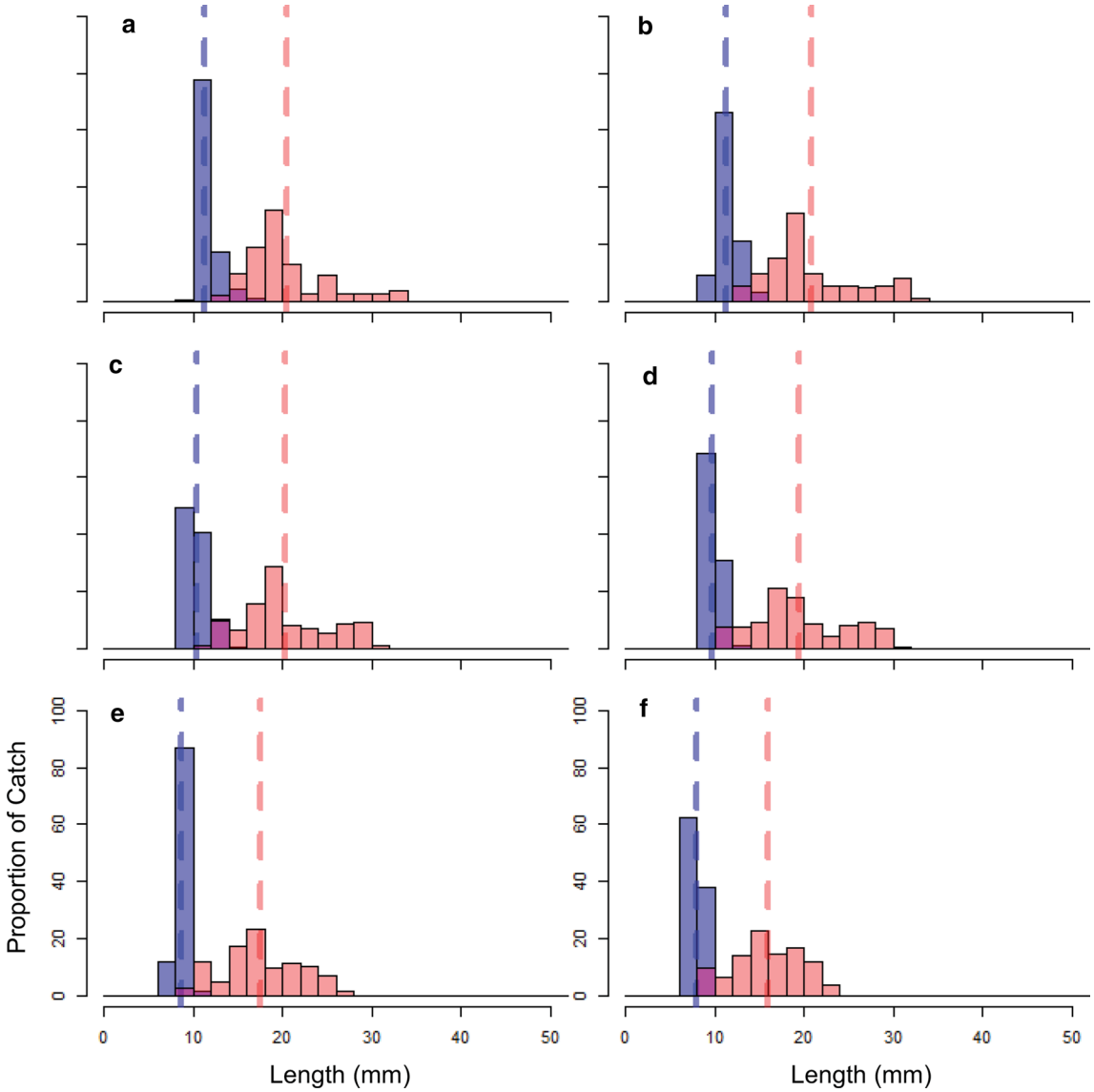

Fig. 7 Length histograms of simulated polar cod (*Boreogadus saida*) larvae by hatch date from the individual-based model in 2017. Hatch dates are: **a** March 1st, **b** March 15th, **c** April 1st, **d** April 15th, **e** May 1st, and **f** May 15th. Blue bars represent late spring (June 19th) lengths and red bars represent late summer (September 1st) lengths. The dashed blue line denotes the mean size of the simulated polar cod in the late spring, whereas the red dashed line denotes the mean size of the simulated polar cod in the late summer. Specimens are binned into 2-mm length intervals

ACC. However, high polar cod abundance in the summer of 2014 corresponded to reduced transport through the Bering Strait (Randall et al. 2019), leading to decreased advection and higher local retention of ELHS. Simulations suggest that polar cod collected along the seafloor and in the water column along the coast and in some offshores areas were likely hatched in Kotzebue Sound and were transported north by the ACC to the northern Chukchi Sea. We believe the likelihood of contamination of polar cod by Arctic cod (*A. glacialis*) is low and not of concern for our analyses. The identity of polar cod collected in the late summer AIES beam trawl was confirmed genetically (S. Wildes, Alaska Fisheries Science Center (AFSC), personal communication). Since the primary currents entering the US Chukchi Sea shelf flow from the south to the north (Danielson et al. 2017), it is unlikely that there is a source of Arctic cod, a high Arctic species, in the southern Chukchi Sea or Bering Strait that would substantially contribute to the larval gadid community of the region (Aschan et al. 2009), especially considering the low sea ice and high water temperatures observed in 2017 (Timmermans et al. 2017; Perovich et al. 2017).

Saffron cod are caught in lower densities than polar cod in the late summer, likely due to their ELHS preferring nearshore habitats not sampled by our surveys (Logerwell

Table 4 Late spring and late summer 2017 simulated length data for polar cod (*Boreogadus saida*) and saffron cod (*Eleginus gracilis*)

Late spring						
	3/1	3/15	4/1	4/15	5/1	5/15
Polar cod	9.8–17.6 (11.3 ± 0.010) *n* = 19,970	9.3–16.7 (11.2 ± 0.0091) *n* = 19,970	8.5–15.1 (10.5 ± 0.0077) *n* = 19,970	7.9–14.1 (9.7 ± 0.0066) *n* = 19,970	7.2–11.7 (8.7 ± 0.0043) *n* = 19,970	6.6–9.7 (7.9 ± 0.0032) *n* = 19,970
Saffron cod	5.1–8.4 (5.7 ± 0.0037) *n* = 19,970	5.1–8.5 (5.7 ± 0.0037) *n* = 19,970	5.1–8.5 (5.7 ± 0.0035) *n* = 19,970	5.1–8.5 (5.7 ± 0.0033) *n* = 19,970	5.1–8.4 (5.7 ± 0.0028) *n* = 19,970	5.1–8.4 (5.6 ± 0.0025) *n* = 19,970
Late summer						
	3/1	3/15	4/1	4/15	5/1	5/15
Polar cod	12.6–33.7 (20.4 ± 0.032) *n* = 19,908	11.4–33.9 (20.8 ± 0.036) *n* = 19,872	10.5–32.0 (20.2 ± 0.034) *n* = 19,895	9.8–30.7 (19.4 ± 0.036) *n* = 19,945	9.1–27.8 (17.6 ± 0.031) *n* = 19,966	8.3–23.5 (15.9 ± 0.026) *n* = 19,947
Saffron cod	9.7–25.3 (14.9 ± 0.023) *n* = 19,919	9.6–25.0 (14.8 ± 0.024) *n* = 19,873	9.6–25.4 (14.7 ± 0.024) *n* = 19,914	9.6–52.7 (14.6 ± 0.024) *n* = 19,940	9.6–35.7 (14.8 ± 0.021) *n* = 19,965	10.7–30.4 (14.9 ± 0.020) *n* = 19,940

Mean size in mm and standard error are reported within the parentheses for each hatching date and sample size (*n*) is reported

et al. 2015; Vestfals et al. 2019). Similar to polar cod, Kotzebue Sound may be a hatching or early nursery area for saffron cod in the late spring. Demersal saffron cod were concentrated in the nearshore, warm waters in northern Kotzebue Sound and around Cape Lisburne, which was similar to the model-predicted distribution, suggesting that saffron cod hatched in Kotzebue Sound were the major source of demersal individuals in the late summer of 2017. Albeit speculative, the few larval saffron cod caught in the water column offshore of Wainwright and Barrow Canyon may be a result of a bet-hedging spawning strategy for saffron cod spawned in Kotzebue Sound and Bering Strait, such as has been documented in other sub-arctic gadids (Laurel et al. 2008; Hutchings and Rangeley 2011). Prolonged hatching periods will result in later hatched saffron cod larvae developing in warmer water where growth rates may be enhanced if mortality related to prey and predators is reduced (Laurel et al. 2008).

Growth and development

The daily growth rates calculated for polar cod and saffron cod were based on individuals collected in the water column and along the bottom using gears that collectively target larvae and juveniles and are used as a coarse estimate of growth in the US Chukchi Sea in the absence of otolith-derived growth rates. Assuming no size-selectivity over the range of sizes that were present, we were able to estimate a range of daily growth rates based on changes in mean length between specimens collected in the late spring and late summer of 2017. Our estimates assume that measured individuals were randomly selected from the same cohort sampled in the late spring and again in the late summer. However, it is probable that individuals from other hatching locations and cohorts were present in the northern Chukchi Sea in the late summer, violating this assumption (e.g., larvae originating from the other side of the U.S. –Russian Federation maritime boundary). In our region in 2017, hatching was observed from January through May, with a peak in April (Z. Chapman, UAF, personal communication), based on the individuals captured during the late spring bongo samples. However, we are likely missing newly hatched larvae in the late spring bongo samples due to the extrusion of these individuals through the 505 µm bongo net mesh (Thanassekos et al. 2012), biasing our samples to individuals that hatched earlier or possessing higher growth rates. The daily growth rate results should be interpreted with caution without a more robust measure of growth using otolith-derived estimates, which is impossible for our study due to our specimens being preserved in formalin at sea. Otolith-derived ages would provide refinement of the length-based daily growth rates estimated in this study by determining individual growth rates and allowing for subsequent exploration of differences in growth trajectories by gear type, sampling season, and region. However, we did account for differences in growth rate by gear type and sampling time by estimating daily growth rates as a range, providing a conservative and a maximal estimate each late summer survey and gear type. Our length-based daily growth estimates also assume a constant growth rate over the sampling season, which is likely violated as individuals attain later stages and larger sizes (Thanassekos and Fortier 2012).

Daily growth estimated in this study for polar cod ranged from 0.27 mm day^{-1} to 0.53 mm day^{-1} with a mean of 0.39 ± 0.06 mm day^{-1} ($n = 4$). Our most conservative

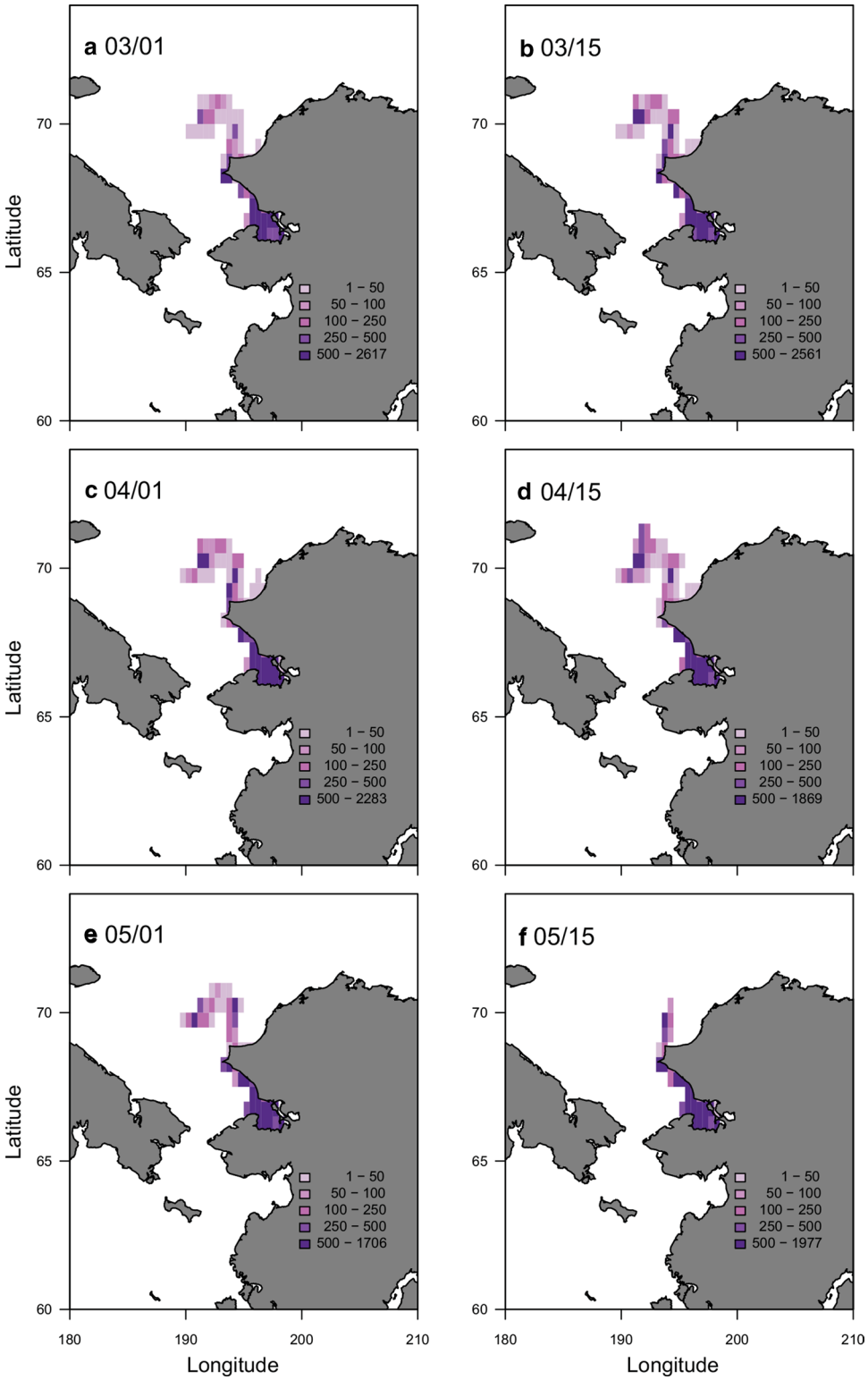

Fig. 8 Density of simulated endpoints from individual-based models in the late spring (June 19th, 2017) for saffron cod (*Eleginus gracilis*) hatching in Kotzebue Sound. Hatch dates are: **a** March 1st, **b** March 15th, **c** April 1st, **d** April 15th, **e** May 1st, and **f** May 15th. Density is calculated in a 0.5 × 0.5 degree grid

growth estimate for polar cod (0.27 mm day^{-1}) agrees well with previous field studies (Bouchard and Fortier 2011; Thanassekos et al. 2012; Vestfals et al. 2019). Daily growth for polar cod in this study may also be higher than is typical due to the elevated water temperatures experienced in 2017. Even though polar cod are adapted to maximize growth at colder temperatures than saffron cod, warmer spring sea surface temperature and earlier ice retreat may be advantageous to larval polar cod due to the availability of zooplankton production supported by earlier

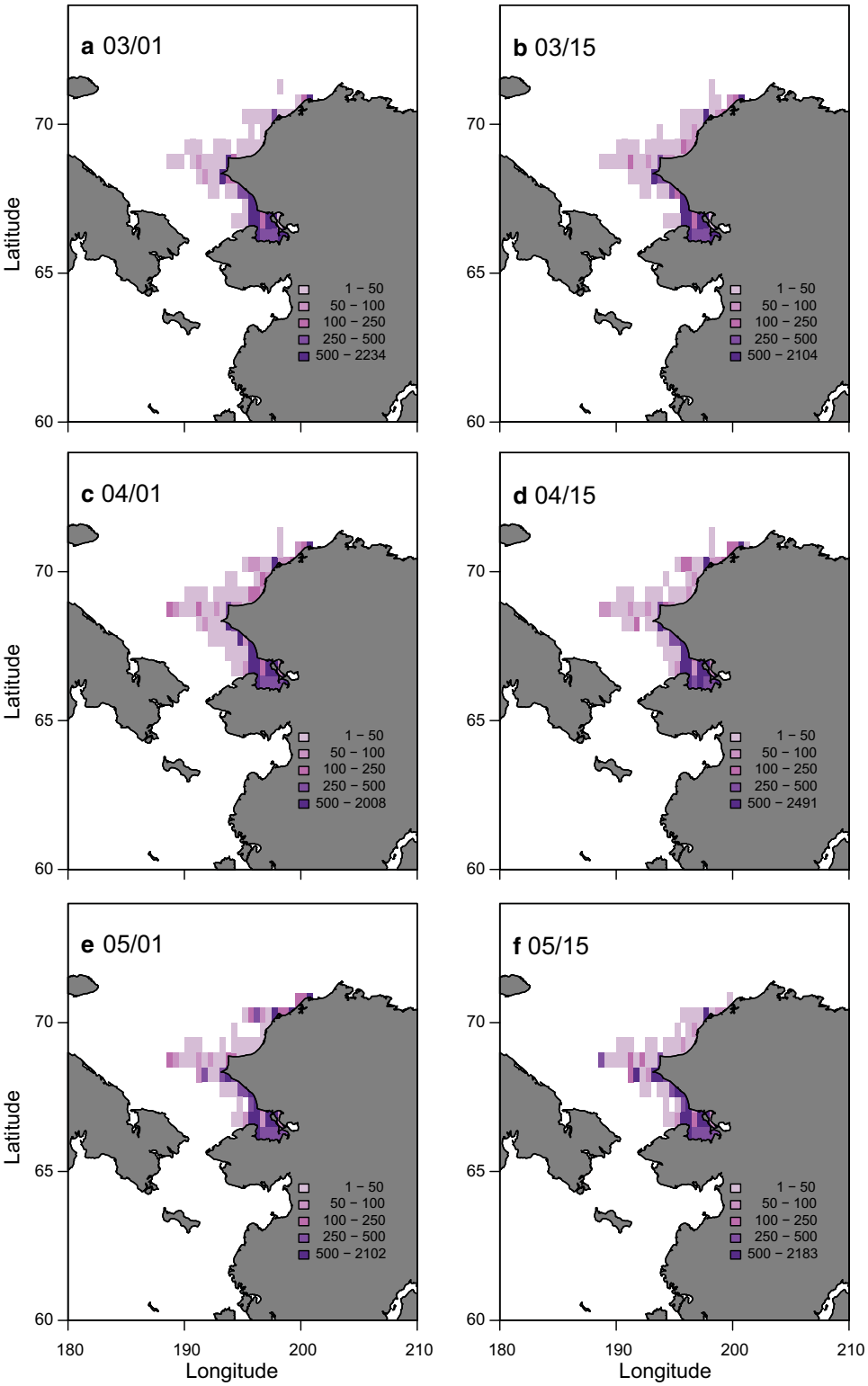

Fig. 9 Density of simulated endpoints from individual-based models in the late summer (September 1st, 2017) for saffron cod (*Eleginus gracilis*) hatched in Kotzebue Sound. Hatch dates are: **a** March 1st, **b** March 15th, **c** April 1st, **d** April 15th, **e** May 1st, and **f** May 15th. Density is calculated in a 0.5 × 0.5 degree grid

ice algae and phytoplankton blooms. This would improve the temporal match of early hatching polar cod with their zooplankton prey (Bouchard et al. 2017). Under scenarios of continued warming in the Arctic, polar cod may lose this growth advantage leading to reduced survival when thermal tolerances of their ELHS are exceeded.

This study is one of the first to estimate daily mean growth for ELHS of saffron cod (0.12–0.76 mm day^{-1};

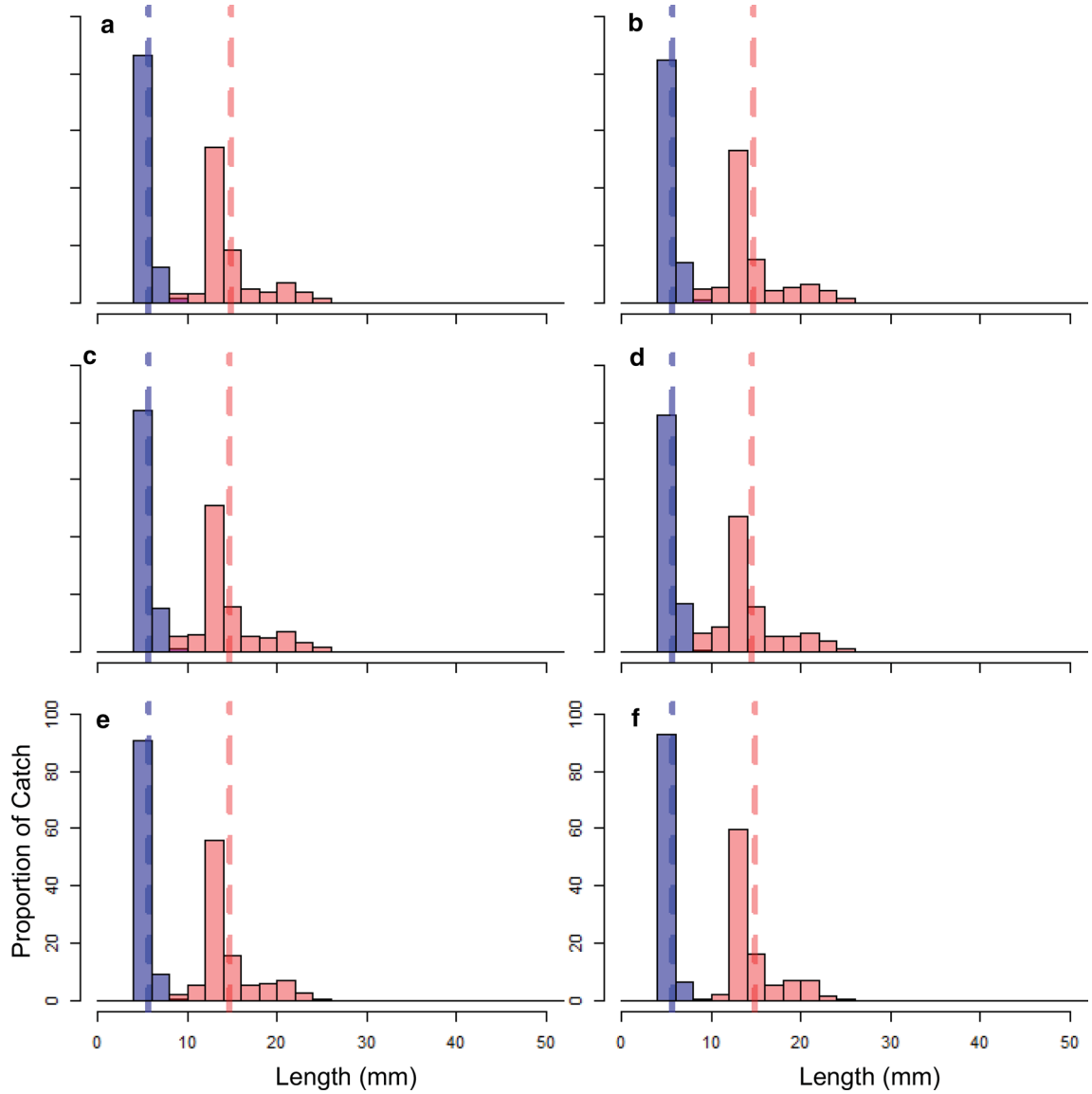

Fig. 10 Length histograms of simulated saffron cod (*Eleginus gracilis*) larvae by hatch date from the individual-based model in 2017. Hatch dates are: **a** March 1st, **b** March 15th, **c** April 1st, **d** April 15th, **e** May 1st, and **f** May 15th. Blue bars represent late spring (June 19th) lengths and red bars represent late summer (September 1st) lengths. The dashed blue line denotes the mean size of the simulated saffron cod in the late spring, whereas the red dashed line denotes the mean size of the simulated saffron cod in the late summer. Specimens are binned into 2-mm length intervals

0.37 ± 0.16 mm day^{-1}; $n = 4$) collected within the Chukchi Sea. The conservative estimate for daily growth for saffron cod was based on bongo collections in the late summer. The lack of larger saffron cod in the bongo gear compared to the mid-water trawl suggests that larger saffron cod were present in the water column, but avoided the bongo net, which targets smaller individuals (De Robertis et al. 2017; Vestfals et al. 2019). A more realistic lower estimate for daily growth was derived from the mid-water IKMT at 0.56 mm day^{-1}. Saffron cod experience faster growth and better condition at higher temperatures than polar cod (Laurel et al. 2016; Vestfals et al. 2019), consistent with larger sizes and higher apparent growth rates in this study, therefore, a warming Arctic may favor saffron cod over polar cod. The growth advantage for saffron cod at higher temperatures may come at the expense of increased metabolic demands and a shift in the zooplankton community to smaller, less lipid-rich copepod species (Copeman et al. 2017; Aarflot et al. 2018; Møller and Nielsen 2020; Bouchard and Fortier 2020).

Model-data comparison

Kotzebue Sound was selected as the source of simulated polar cod and saffron cod ELHS in this study due to the preponderance of small larvae observed in this area in the late spring, highlighting the region's potential role as a key hatching and/or nursery habitat for the ELHS of these species. The observed distribution of Arctic gadids along the northern coastline of Kotzebue Sound in the late spring matched well with simulated larval distributions from the model. At Point Hope and Cape Lisburne, a portion of the ACC is often deflected offshore (Danielson et al. 2017), which is reflected in both the late spring model simulations and survey catch data. The IBM predicts that larval polar cod and saffron cod will be advected offshore and northward at Cape Lisburne. Consistent with the model simulations, we observed high catches of polar cod and saffron cod offshore of Cape Lisburne during the spring survey. High abundances of polar cod and saffron cod may also be present north of Cape Lisburne in the spring as predicted by the IBM, but we lack the empirical data to test this as sampling did not extend north of Cape Lisburne. Additionally, the simulated distributions for saffron cod and polar cod from the IBM were similar to each other. This is due to the use of a single release location (Kotzebue Sound) for both species and identical behavior routines so that differences in distribution in our study were associated with the species-specific temperature-dependent growth rates used to parametrize the IBMs (Vestfals et al. 2021).

There was no evidence from the model that larvae are advected south from Kotzebue Sound. Any spawning in Kotzebue Sound is likely not the origin of individuals that were caught around St. Lawrence Island or nearshore along the northern Seward Peninsula during spring. Recent modeling work suggests that polar cod hatching south of Bering Strait could be the source of larvae and early juveniles encountered in surveys in the northeastern Chukchi Sea in 2012 while Bering Strait and Kotzebue Sound were likely source regions for saffron cod in 2012 and 2013 (Vestfals et al. 2021).

In the late summer, the IBMs for polar cod and saffron cod indicated high concentrations of larvae and early juveniles nearshore from northern Kotzebue Sound to Wainwright, offshore of Point Hope/Cape Lisburne, and offshore of Wainwright. The modeled distributions agree with the observed late summer distribution of saffron cod where higher abundances were generally nearshore, especially around Point Hope and Cape Lisburne, with abundance decreasing offshore. This suggests that Kotzebue Sound is a center of abundance and potentially serves as an important spawning and hatching area for saffron cod in the Chukchi Sea, a possibility that has been suggested anecdotally (A. Whiting, Village of Kotzebue, personal communication; Vestfals et al. 2021). Larval polar cod were ubiquitous offshore in the Hanna Shoal region during the late summer surveys in 2017, which is consistent with polar cod distributions in other years (Logerwell et al. 2020), but was not captured well by the model, indicating that other hatching locations are major contributors to the observed age-0 aggregations in this area (Vestfals et al. 2021). The simulated distribution overlapped with the distribution of late summer polar cod ELHS individuals offshore of Point Hope and Cape Lisburne, as well as nearshore extending from Cape Lisburne to Wainwright, suggesting Kotzebue Sound may be a potential source of polar cod to these areas in the late summer.

Simulated lengths for both polar cod and saffron cod were smaller than observed specimens collected in the late spring and late summer from the water column or the bottom, with a much larger discrepancy for saffron cod than polar cod. This suggests that the model is underestimating growth, small larvae in the field experience higher mortalities than large larvae, temperatures in the model are underestimates, hatching occurs earlier than assumed, or a combination of these and potentially other factors. The growth equations for polar cod and saffron cod within the IBM are temperature-mediated (Vestfals et al. 2021), making simulated lengths and estimates of daily growth sensitive to thermal conditions in the model, which may differ from those experienced in the field. No growth model exists for ELHS of saffron cod larger than 10 mm in length and the growth model was parameterized using data for walleye pollock due to their similar, linear growth trajectories prior to 10 mm (B. Laurel, AFSC, personal communication; Porter and Bailey 2007; Petrik et al. 2015). However, saffron cod may deviate from linear growth trajectories at later stages or temperatures (Vestfals et al. 2021). Additionally, field estimates of apparent growth tend to be higher than those observed in the lab because of ecological interactions, such as size-selective predation (Houde 2009). The field-based growth calculations were relatively coarse, encompassing all the collected individuals aggregated from a large spatial area, over a two-month sampling period, and likely originating from multiple spawn locations, whereas the model is based on a single release location.

In the late spring, simulated polar cod hatched before April 15th were larger on average than the individuals captured from the water column, suggesting the model is realistically reflecting the enhanced growth rates of polar cod in the late spring due to earlier ice retreat and warmer water temperatures in 2017 relative to average conditions. The narrow size range of individuals in the model compared to the field collections can indicate several potential scenarios. Firstly, Kotzebue Sound was selected as the source of polar cod and saffron cod larvae, but it is not the only source of larvae in the Chukchi Sea. For example, recent modeling work suggests that Bering Strait and Chukotka

Peninsula were important hatching areas for polar cod in the Chukchi Sea in 2012 and 2013 (Vestfals et al. 2021). Secondly, the presence of smaller polar cod in the catch in the late spring may also suggest a simulated hatch date of April 15th or later, although the model does not capture the full range of observed sizes, particularly at the upper end. We selected to model hatch dates between March 1st and May 15th, which corresponded to the duration of peak hatching for polar cod in 2017, although hatching has been reported as early as January 1st for polar cod in the Arctic (Bouchard and Fortier 2011; Z. Chapman, UAF, personal communication). In polar cod, hatch date explains more variability in length than temperature conditions (Bouchard et al. 2017), therefore, some of the inconsistencies between the sizes, and subsequent calculated growth rates, of field collected and simulated individuals may be due to the hatch date variability. Thirdly, field estimates also differ from those observed under controlled laboratory conditions due to ecological factors that are difficult to account for (Bailey and Houde 1989; Houde 2009; Vestfals et al. 2019) such as patchy prey distribution and small-scale environmental variability (temperature, salinity, etc.). Polar cod are likely able to take advantage of a "big risk, big reward" strategy to forage for limited periods of time in warm, productive waters along thermal-salinity fronts to maximize growth relative to conspecifics (Laurel et al. 2016; Bouchard et al. 2017), which may contribute to the wider size range observed for the field-collected individuals compared to simulated individuals in the late spring.

Differences between simulated and empirical data may also be related to the onset of demersal behavior in polar cod and saffron cod, which is an adaptation to avoid predation, enhance foraging, and find areas of physiological preferred temperature ranges. Given the dominance of gadids by number and biomass in demersal catches in the Arctic (Logerwell et al. 2015), fish predators of ELHS of polar cod and saffron cod are likely conspecifics. Cannibalism has been documented in other subarctic gadids and is mitigated by vertical partitioning between juveniles and adults (Bailey 1975, 1989). Adult walleye pollock in the Bering Sea are semipelagic and cannibalism was highest when juveniles moved deeper in the water column, overlapping with the adults (Bailey 1989). Cannibalism is considered rare for polar cod due to their planktivorous foraging strategy, although fishes do become an important prey category as polar cod grow, and instances of cannibalism have been documented (Bain and Sekerak 1978; Benoit et al. 2010; Christiansen et al. 2012; Whitehouse et al 2017). Polar cod forage primarily on copepod nauplii (e.g., *Pseudocalanus* spp.) when smaller than 25 mm SL and shift to foraging on the copepodite stages of copepods, specifically *Calanus* spp. and *Metridia* spp., and fishes when larger than 25 mm SL (Benoit et al. 2010; Christiansen et al. 2012; Bouchard et al. 2016; Bouchard and Fortier 2020). Saffron cod likely become more piscivorous with increasing size (Laurel et al. 2009), suggesting cannibalism may be more likely in this species than polar cod. Diet data are limited for saffron cod in the Chukchi Sea (Copeman et al. 2016). Increased water temperatures and constriction of available habitat for Arctic taxa may lead to increased cannibalism for polar cod and saffron cod as well as increased competition and predation if subarctic species move into the Chukchi Sea (Bouchard et al. 2017). A number of adult fish species from the Bering Sea, such as walleye pollock and Pacific cod, expanded northward in response to a reduced Cold Pool (bottom water temperatures < 2 °C) over the Bering Sea shelf (Stevenson and Lauth 2019) and are possible competitors as well as predators of Arctic gadids in the Chukchi Sea if climatic warming persists (Marsh and Mueter 2019). Near bottom waters may also act as a thermal refuge for smaller Arctic gadids, particularly small polar cod that are not as tolerant to higher water temperatures as saffron cod (Laurel et al. 2016).

Summary

The late spring distributions of polar cod and saffron cod centered in Kotzebue Sound suggest that sea ice may be an important environmental factor influencing hatching, and it may provide a nursery habitat for newly hatched individuals of both species. Kotzebue Sound was likely a source of ELHS of polar cod and saffron cod offshore of Point Hope/Cape Lisburne and nearshore from Kotzebue Sound to Wainwright during 2017. Without otolith-derived individual growth estimates, it is difficult to know if polar cod and saffron cod experienced greater growth during 2017 compared to other years or regions due to elevated temperatures, although our daily growth estimates were higher than reported in past research (Bouchard and Fortier 2011). Saffron cod should benefit in a warmer Arctic if their ELHS are resilient to the loss of sea ice, and if energetic trade-offs can offset prey-mediated factors that may depress growth (i.e., reduced nutritional value, zooplankton community shift) (Llopiz et al. 2014; Spear et al. 2019) and an increase in competition and predation from sub-Arctic demersal fishes shifting to the north (Stevenson and Lauth 2019). With the forecasted warming in the Arctic and projected changes in sea ice dynamics, studies such as this one synthesizing the seasonal distribution, abundance, and growth of Arctic forage fishes are critical to assess changes in phenology, distributions, and abundance for these species and the impacts of warming on habitat availability for Arctic fishes.

Acknowledgements The authors thank all of the boat and field crews of the USCGC *Healy*, M/V *Ocean Starr*, and R/V *Sikuliaq* who collected these data and without their tireless efforts, this project would not have been possible. We thank the Plankton Sorting and Identification Center in Szczecin, Poland and the ichthyoplankton team at

the Alaska Fisheries Science Center for their taxonomic expertise that makes studies of the ecology of Arctic fishes possible. We also thank Jens Nielsen and Adam Spear for their assistance gathering and plotting the sea ice data as well as intellectual discussions on the interpretation of the data. Finally, we thank Katherine Hedstrom at the University of Alaska Fairbanks for providing the PAROMS model output and Caitlin Smoot and Cheryl Hopcroft, also at the University of Alaska Fairbanks, for facilitating data collection and curation of ASGARD samples. Funding for this project was provided by the North Pacific Research Board through the Arctic Integrated Ecosystem Research Program. AMBON collections were made possible through a National Ocean Partnership Program (NOPP Grant NA14NOS0120158) by the National Oceanic and Atmospheric Administration, the Bureau of Ocean Management and Shell Exploration & Production. The findings and conclusions in the paper are those of the author(s) and do not necessarily represent the views of the National Marine Fisheries Service. Mention of trade names does not imply endorsement by NOAA or any of its subagencies. This is contribution number EcoFOCI-1015 of Ecosystems and Fisheries-Oceanography Coordinated Investigations.

Author contributions ALD, EAL, EDG, and JTD conceived and framed the key questions of the study. CDV conducted all IBM analyses, contributed code to generate figures related to the IBM, and provided text in the *Methods* sections. FJM, SLD, EAL, and RRH provided data that made the analyses possible. ALD wrote the manuscript and generated the figures. All authors read and approved the manuscript.

Declarations

Conflict of interest The authors have no conflict of interest to report.

Ethical approval All field sampling was done in accordance with NOAA NMFS policies, as outlined under the Animal Welfare Act and US Government Principles for the Utilization and Care of Vertebrate Animals Used in Testing, Research, and Training. Collections were made under the following permits approved by the Alaska Regional Office, National Marine Fisheries Service (CF-17-023), a US Fish and Wildlife Service Seabird Salvage Permit (MB035470), and a State of Alaska Resource Permit (CF-16-010).

References

Abookire AA, Rose CS (2005) Modifications to a plumb staff beam trawl for sampling uneven, complex habitats. Fish Res 71:247–254. https://doi.org/10.1016/j.fishres.2004.06.006

Cavalieri DJ, Parkinson CL, Gloersen P, Zwally HJ (1996) Sea Ice Concentrations from Nimbus-7 SMMR and DMSP SSM/I-SSMIS Passive Microwave Data, Version 1. Boulder, Colorado USA. NASA National Snow and Ice Data Center Distributed Active Archive Center. https://doi.org/10.5067/8GQ8LZQVL0VL. [10 April 2019].

Aarflot JM, Skjoldal HR, Dalpadado P, Skern-Mauritzen M (2018) Contribution of *Calanus* species to the mesozooplankton biomass in the Barents Sea. ICES J Mar Sci 75(7):2342–2354

Aschan M, Karamushko OV, Byrkjedal I, Wienerroither R, Borkin IV, Christiansen JS (2009) Records of the gadoid fish *Arctogadus glacialis* (Peters, 1874) in the European Arctic. Polar Biol 32(7):963–970

Bailey RS (1975) Observations on diel behaviour patterns of North Sea gadoids in the pelagic phase. J Mar Biol Assoc UK 55(1):133–142

Bailey KM (1989) Interaction between the vertical distribution of juvenile walleye pollock *Theragra chalcogramma* in the eastern Bering Sea, and cannibalism. Mar Ecol Prog Ser 53:205–213

Bailey KM, Houde ED (1989) Predation on egg and larvae of marine fishes and the recruitment problem. Adv Mar Biol 25:1–83

Bain H, Sekerak AD (1978) Aspects of the biology of Arctic cod (*Boreogadus saida*) in the central Canadian Arctic. LGL Limited, Toronto

Benoit D, Simard Y, Gagne J, Geoffroy M, Fortier L (2010) From polar night to midnight sun: photoperiod, seal predation, and the diel vertical migrations of polar cod (*Boreogadus saida*) under landfast ice in the Arctic Ocean. Polar Biol 33:1505–1520. https://doi.org/10.1007/s00300-010-0840-x

Borkin LV, Ozhigin VK, Shleinik VN (1986) Effect of oceanographical factors on the abundance of the Barents Sea polar cod year classes. In: The effect of oceanographic conditions on distribution and population dynamics of commercial fish stocks in the Barents Sea, vol 169

Bouchard C, Fortier L (2008) Effects of polynyas on the hatching season, early growth and survival of polar cod *Boreogadus saida* in the Laptev Sea. Mar Ecol Prog Ser 355:247–256. https://doi.org/10.3354/meps07335

Bouchard C, Fortier L (2011) Circum-arctic comparison of the hatching season of polar cod *Boreogadus saida*: a test of the freshwater winter refuge hypothesis. Prog Oceanogr 90:105–116. https://doi.org/10.1016/j.pocean.2011.02.008

Bouchard C, Fortier L (2020) The importance of *Calanus glacialis* for the feeding success of young polar cod: a circumpolar synthesis. Polar Biol. https://doi.org/10.1007/s00300-020-02643-0

Bouchard C, Mollard S, Suzuki K, Robert D, Fortier L (2016) Contrasting the early life histories of sympatric Arctic gadids *Boreogadus saida* and *Arctogadus glacialis* in the Canadian Beaufort Sea. Polar Biol 39:1005–1022. https://doi.org/10.1007/s00300-014-1617-4

Bouchard C, Geoffroy M, Leblanc M, Majewski A, Gautheir S, Walkusz W, Reist JD, Fortier L (2017) Climate warming enhances polar cod recruitment, at least transiently. Prog Oceanogr 156:121–129. https://doi.org/10.1016/j.pocean.2017.06.008

Budgell WP (2005) Numerical simulation of ice-ocean variability in the Barents Sea region. Ocean Dyn 55:370–387. https://doi.org/10.1007/s10236-005-0008-3

Carton JA, Chepurin GA, Chen L (2018) SODA3: a new ocean climate reanalysis. J Clim 31(17):6967–6983

Chassignet EP, Hurlburt HE, Metzger EJ, Smedstad OM, Cummings JA, Halliwell GR, Bleck R, Baraille R, Wallcraft AJ, Lozano C, Tolman HL, Srinivasan A, Hankin S, Cornillon P, Weisberg R, Barth A, He R, Werner F, Wilkin J (2009) US GODAE global ocean prediction with the hybrid coordinate ocean model (HYCOM). Oceanography 22:49–59

Christiansen JS, Hop H, Nilssen EM, Joensen J (2012) Trophic ecology of sympatric Arctic gadoids, *Arctogadus glacialis* (Peters, 1872) and *Boreogadus saida* (Lepechin, 1774), in NE Greenland. Polar Biol 35:1247–1257. https://doi.org/10.1007/s00300-012-1170-y

Copeman LA, Laurel BJ, Boswell KM, Sremba AL, Klinck K, Heintz RA, Vollenweider JJ, Helser TE, Spencer ML (2016) Ontogenetic and spatial variability in trophic biomarkers of juvenile saffron cod (*Eleginus gracilis*) from the Beaufort, Chukchi and Bering Seas. Polar Biol 39:1109–1126. https://doi.org/10.1007/s00300-015-1792-y

Copeman LA, Laurel BJ, Spencer M, Sremba A (2017) Temperature impacts on lipid allocation among juvenile gadid species at the Pacific Arctic-Boreal interface: an experimental laboratory approach. Mar Ecol Prog Ser 566:183–198. https://doi.org/10.3354/meps12040

Craig PC, Griffiths WB, Haldorson L, McElderry H (1982) Ecological studies of Arctic cod (*Boreogadus saida*) in Beaufort Sea Coastal

Waters, Alaska. Can J Fish Aquat Sci 39:395–406. https://doi.org/10.1139/f82-057
Danielson SL, Eisner L, Ladd C, Mordy C, Sousa L, Weingartner TJ (2017) A comparison between late summer 2012 and 2013 water masses, macronutrients, and phytoplankton standing crops in the northern Bering and Chukchi Seas. Deep Sea Res Part II 135:7–26. https://doi.org/10.1016/j.dsr2.2016.05.024
Danielson SL, Hedstrom KS, Weingartner TJ (2016) Bering-Chukchi circulation pathways, North Pacific Research Board 2016 Final Report, NPRB project #1308, University of Alaska Fairbanks, Fairbanks, AK
De Robertis A, Taylor K, Williams K, Wilson CD (2017) Species and size selectivity of two midwater trawls used in an acoustic survey of the Alaska Arctic. Deep Sea Res Part II 135:40–50
Döös K (1995) Interocean exchange of water masses. J Geophys Res 100:13499. https://doi.org/10.1029/95jc00337
Dunn JR, Vinter BM (1984) Development of larvae of the saffron cod, *Eleginus gracilis*, with comments on the identification of gadid larvae in Pacific and Arctic waters contiguous to Canada and Alaska. Can J Fish Aquat Sci 41:304–318
Egbert GD, Erofeeva SY (2002) Efficient inverse modeling of barotropic ocean tides. J Atmos Ocean Technol 19:183–204. https://doi.org/10.1175/1520-0426(2002)019%3c0183:EIMOBO%3e2.0.CO;2
Falardeau M, Bouchard C, Robert D, Fortier L (2017) First records of Pacific sand lance (*Ammodytes hexapterus*) in the Canadian Arctic Archipelago. Polar Biol 40:2291–2296. https://doi.org/10.1007/s00300-017-2141-0
Graham RM, Cohen L, Petty AA, Boisvert LN, Rinke A, Hudson SR, Nicolaus M, Granskog MA (2017) Increasing frequency and duration of Arctic winter warming events. Geophys Res Lett 44:6974–6983. https://doi.org/10.1002/2017GL073395
Grebmeier JM, Bluhm B, Cooper LW (2015) Time-Series benthic community composition and biomass and associated environmental characteristics in the Chukchi Sea during the RUSALCA 2004–2012 program. Oceanography 28(3):116–133. https://doi.org/10.5670/oceanog.2015.61
Helser TE, Colman JR, Anderl DM, Kastelle CR (2017) Growth dynamics of saffron cod (*Eleginus gracilis*) and Arctic cod (*Boreogadus saida*) in the Northern Bering and Chukchi Seas. Deep Sea Res Part II 135:66–77. https://doi.org/10.1016/j.dsr2.2015.12.009
Houde ED (2009) Recruitment variability. In: Jakobsen T, Fogarty M, Megrey B, Moksness E (eds) Reproductive biology of fishes: implications for assessment and management. Wiley-Blackwell, Oxford, pp 91–171
Hunt GL, Blanchard AL, Boveng P, Dalpadado P, Drinkwater KF, Eisner L, Hopcroft RR, Kovacs KM, Norcross BL, Renaud P, Reigstad M, Renner M, Skjoldal HR, Whitehouse A, Woodgate RA (2013) The Barents and Chukchi Seas: comparison of two Arctic shelf ecosystems. J Mar Syst 109–110:43–68. https://doi.org/10.1016/j.jmarsys.2012.08.003
Hutchings JA, Rangeley RW (2011) Correlates of recovery for Canadian Atlantic cod (*Gadus morhua*). Can J Zool 89:386–400. https://doi.org/10.1139/Z11-022
Kahru M, Brotas V, Manzano-Sarabia M, Mitchell BG (2011) Are phytoplankton blooms occurring earlier in the Arctic? Glob Chang Biol 17:1733–1739. https://doi.org/10.1111/j.1365-2486.2010.02312.x
Koenker BL, Copeman LA, Laurel BJ (2018) Impacts of temperature and food availability on the condition of larval Arctic cod (*Boreogadus saida*) and walleye pollock (*Gadus chalcogrammus*). ICES J Mar Sci 75(7):2370–2385. https://doi.org/10.1093/icesjms/fsy052
Laurel BJ, Hurst TP, Copeman LA, Davis MW (2008) The role of temperature on the growth and survival of early and late hatching Pacific cod larvae (*Gadus macrocephalus*). J Plankton Res 30:1051–1060. https://doi.org/10.1093/plankt/fbn057
Laurel BJ, Ryer CH, Knoth B, Stoner AW (2009) Temporal and ontogenetic shifts in habitat use of juvenile Pacific cod (*Gadus macrocephalus*). J Exp Mar Bio Ecol 377:28–35. https://doi.org/10.1016/j.jembe.2009.06.010
Laurel BJ, Spencer M, Iseri P, Copeman LA (2016) Temperature-dependent growth and behavior of juvenile Arctic cod (*Boreogadus saida*) and co-occurring North Pacific gadids. Polar Biol 39:1127–1135. https://doi.org/10.1007/s00300-015-1761-5
Li WKW, McLaughlin FA, Lovejoy C, Carmack EC (2009) Smallest algae thrive as the Arctic ocean freshens. Science 326:539. https://doi.org/10.1126/science.1179798
Llopiz JK, Cowen RK, Hauff MJ, Ji R, Munday PL, Muhling BA, Peck MA, Richardson DE, Sogard S, Sponaugle S (2014) Early life history and fisheries oceanography: new questions in a changing world. Oceanography 27(4):26–41
Logerwell E, Busby M, Carothers C, Cotton S, Duffy-Anderson J, Farley E, Goddard P, Heintz R, Holladay B, Horne J, Johnson S, Lauth B, Moulton L, Neff D, Norcross B, Parker-Stetter S, Seigle J, Sformo T (2015) Fish communities across a spectrum of habitats in the western Beaufort Sea and Chukchi Sea. Prog Oceanogr 136:115–132. https://doi.org/10.1016/j.pocean.2015.05.013
Logerwell E, Busby M, Mier K, Tabisola H, Duffy-Anderson J (2020) The effects of oceanographic variability on the distribution of larval fishes of the northern Bering and Chukchi Seas. Deep Sea Res Part II. https://doi.org/10.1016/j.dsr2.2020.104784
Lønne OJ, Gulliksen B (1989) Size, age and diet of polar cod, *Boreogadus saida* (Lepechin 1773), in ice covered waters. Polar Biol 9(3):187–91
Marsh JM, Mueter FJ (2019) Influences of temperature, predators, and competitors on polar cod (*Boreogadus saida*) at the southern margin of their distribution. Polar Biol 35:1–20. https://doi.org/10.1007/s00300-019-02575-4
Maslowski W (2014) The pacific arctic region: ecosystem status and trends in a rapidly changing environment. In: Grebmeier JM, Maslowski W (eds) The Pacific Arctic region. Springer, Heidelberg, pp 101–132
Matarese A, Kendall A, Blood D, Vinter B (1989) Laboratory guide to early life history stages of northeast Pacific fishes. NOAA Tech Rep 80:652
Møller EF, Nielsen TG (2020) Borealization of Arctic zooplankton—smaller and less fat zooplankton species in Disko Bay. Western Greenland Limnol Oceanogr 65(6):1175–1188
National Snow and Ice Data Center (NSIDC) (2019) All About Sea Ice. Accessed 15 June 2019. /cryosphere/seaice/index.html
North Pacific Fishery Management Council (NPFMC) (2009) Fishery Management Plan for Fish Resources of the Arctic Management Area. North Pacific Fishery Management Council, Anchorage, AK
Ichthyoplankton Information System (IIS) (2019) National Oceanic and Atmospheric Administration. (7 May 2020) https://apps-afsc.fisheries.noaa.gov/ichthyo/index.php
Overland JE, Wang M, Ballinger TJ (2018) Recent increased warming of the Alaskan marine Arctic due to midlatitude linkages. Adv Atmos Sci 35:75–84. https://doi.org/10.1007/s00376-017-7026-1
Perovich D, Meier W, Tschudi M, Farrell S, Hendricks S, Gerland S, Haas C, Krumpen T, Polashenski C, Ricker R, Webster M (2017). Sea Ice [in Arctic Report Card 2017]. http://www.arctic.noaa.gov/Report-Card
Petrik CM, Duffy-Anderson JT, Mueter F, Hedstrom K, Curchitser EN (2015) Biophysical transport model suggests climate variability determines distribution of Walleye Pollock early life stages in the eastern Bering Sea through effects on spawning. Progr Oceanogr 138:459–474

Porter SM, Bailey KM (2007) The effect of early and late hatching on the escape response of walleye pollock (*Theragra chalcogramma*) larvae. J Plankton Res 29:291–300. https://doi.org/10.1093/plankt/fbm015

R Core Team (2019) R: a language and environment for statistical computing. R Foundation for Statistical Computing, Vienna, Austria. ISBN 3-900051-07-0, http://www.Rproject.org

Randall JR, Busby MS, Spear AH, Mier KL (2019) Spatial and temporal variation of summer ichthyoplankton assemblage structure in the eastern Chukchi Sea 2010–2015. Polar Biol 42:1811–1824

Rass TS (1968) Spawning and development of polar cod. Rapp PV Reun Cons Perm Int Explor Mer 158:135–137

Shchepetkin AF, McWilliams JC (2005) The regional oceanic modeling system (ROMS): a split-explicit, free-surface, topography-following-coordinate oceanic model. Ocean Model 9:347–404. https://doi.org/10.1016/j.ocemod.2004.08.002

Shima M, Bailey KM (1994) Comparative analysis of ichthyoplankton sampling gear for early life stages of walleye pollock (*Theragra chalcogramma*). Fish Oceanogr 3:50–59. https://doi.org/10.1111/j.1365-2419.1994.tb00047.x

Spear A, Duffy-Anderson J, Kimmel D, Napp J, Randall J, Stabeno P (2019) Physical and biological drivers of zooplankton communities in the Chukchi Sea. Polar Biol 42:1107–1124. https://doi.org/10.1007/s00300-019-02498-0

Stevenson DE, Lauth RR (2019) Bottom trawl surveys in the northern Bering Sea indicate recent shifts in the distribution of marine species. Polar Biol 42:407–421. https://doi.org/10.1007/s00300-018-2431-1

Thanassekos S, Fortier L (2012) An individual based model of Arctic cod (*Boreogadus saida*) early life in Arctic polynyas: I. Simulated growth in relation to hatch date in the Northeast Water (Greenland Sea) and the North Water (Baffin Bay). J Mar Syst 93:25–38

Thanassekos S, Robert D, Fortier L (2012) An individual based model of Arctic cod (*Boreogadus saida*) early life in Arctic polynyas: II. Length-dependent and growth-dependent mortality. J Mar Syst 93:39–46

Timmermans ML, Ladd C, Wood K (2017) Sea surface temperature [in Arctic Report Card 2017]. http://www.arctic.noaa.gov/Report-Card

Tokinaga H, Xie S-P, Mukougawa H (2017) Early 20th-century Arctic warming intensified by Pacific and Atlantic multidecadal variability. Proc Natl Acad Sci USA 114:6227–6232. https://doi.org/10.1073/pnas.1615880114

Tsujino H, Urakawa S, Nakano H, Small RJ, Kim WM, Yeager SG, Danabasoglu G, Suzuki T, Bamber JL, Bentsen M, Böning CW (2018) JRA-55 based surface dataset for driving ocean–sea-ice models (JRA55-do). Ocean Model 130:79–139

Vestfals CD, Mueter FJ, Duffy JT, Busby MS, De Robertis A (2019) Spatio-temporal distribution of polar cod (*Boreogadus saida*) and saffron cod (*Eleginus gracilis*) early life stages in the Pacific Arctic. Polar Biol 42(5):969–990. https://doi.org/10.1007/s00300-019-02494-4

Vestfals CD, Mueter FJ, Hedstrom KS, Laurel BJ, Petrik CM, Duffy-Anderson JT, Danielson SL (2021) Modeling the dispersal of polar cod (*Boreogadus saida*) and saffron cod (*Eleginus gracilis*) early life stages in the Pacific Arctic using a biophysical transport model. Prog Oceanogr. https://doi.org/10.1016/j.pocean.2021.102571

Whitehouse GA, Aydin K, Essington TE (2014) A trophic mass balance model of the eastern Chukchi Sea with comparisons to other high-latitude systems. Ocean Model 88:911–939. https://doi.org/10.1007/s00300-014-1490-1

Whitehouse GA, Buckley TW, Danielson SL (2017) Diet compositions and trophic guild structure of the eastern Chukchi Sea demersal fish community. Deep Sea Res Part II 135:95–110

Wildes SL, Whittle J, Nguyen H, Guyon J (2016) *Boreogadus saida* genetics in the Alaskan Arctic. US Dept. of the Interior, Bureau of Ocean Energy Management, Alaska OCS Region. OCS Study BOEM 2011-AK-11-08 a/b. 67 pp—DRAFT REPORT

Wolotira RJ Jr (1985) Saffron cod (*Eleginus gracilis*) in Western Alaska: the resource and its potential. U.S. Dep. Commer., NOAA Tech. Memo. F/NWC-79. 119 p

Woodgate RA (2018) Increases in the Pacific inflow to the Arctic from 1990 to 2015, and insights into seasonal trends and driving mechanisms from year-round Bering Strait mooring data. Prog Oceanogr 160:124–154

Woodgate RA, Weingartner TJ, Lindsay R (2012) Observed increases in Bering Strait oceanic fluxes from the Pacific to the Arctic from 2001 to 2011 and their impacts on the Arctic Ocean water column. Geophys Res Lett. https://doi.org/10.1029/2012GL054092